TOPOLOGY DESIGN USING B-SPLINE FINITE ELEMENTS

By

ANAND PARTHASARATHY

A THESIS PRESENTED TO THE GRADUATE SCHOOL
OF THE UNIVERSITY OF FLORIDA IN PARTIAL FULFILLMENT
OF THE REQUIREMENTS FOR THE DEGREE OF
MASTER OF SCIENCE

UNIVERSITY OF FLORIDA

2010

To my parents, Parthasarathy and Ramamani Parthasarathy, my advisors, Dr. Ashok V. Kumar, Dr. Raphael T. Haftka, Dr. Bhavani V. Sankar, and my other close family members, relatives and friends

ACKNOWLEDGMENTS

I would like to thank and express my sincere gratitude to Dr. Ashok V. Kumar, chairman and advisor for my thesis committee, for his visionary guidance, invaluable insights, encouragement and support throughout the period of my research work. He played a pivotal role to take the thesis to the current form it is and it would have been virtually impossible to complete this thesis without his invaluable inputs.

I would also like to extend my sincere thanks to the other members of the supervisory committee, Dr. Raphael T. Haftka and Dr. Bhavani V. Sankar for their constant support, help whenever required and invaluable suggestions during the review process. It is my privilege to have such enlightened people on my thesis committee.

I would like to thank Mr. Parthasarathy, Mrs. Ramamani Parthasarathy, Anusha, Mr. and Mrs. Narayanan, Mr. and Mrs. Srinivasan, Mr. and Mrs. T.S. Venkatakrishnan, Mr. and Mrs. Ramanathan, Mr. and Mrs. Sundararaman, Mr. and Mrs. AnanthaKrishnan, Mr. and Mrs. Venkatraman, Mr. and Mrs Ravi, Mr. and Mrs. Sundaram, Sivasubramanian, Shankar, Srikanth, Chandru, Ramprasad, Toral, Chandrasekar, Prasanna and Karthik MM for their moral support and innumerable help. I would like to thank University of Florida for their help and support. I would like to thank my lab mates Prem Dheepak, Mittu Pannala and Sung Uk Zhang for their help and support. Finally, I would like to express my gratitude and thanks to God for giving me this wonderful opportunity.

TABLE OF CONTENTS

page

ACKNOWLEDGMENTS 4

LIST OF TABLES 7

LIST OF FIGURES 8

ABSTRACT 10

CHAPTER

1 INTRODUCTION 12

Overview 12
Goals and Objectives 16
Outline 17

2 TOPOLOGY OPTIMIZATION 19

Introduction 19
Sizing Optimization 19
Shape Optimization 20
Topology Optimization 24
Topology Optimization Methods 25
Homogenization Method 27
Solid Isotropic Material with Penalization 29

3 B-SPLINE FINITE ELEMENTS 35

Introduction 35
B-spline Elements 36
Merits and Demerits of B-spline Elements 43
Implicit Boundary Finite Element Method 44
Solution Structure 44
Dirichlet Functions 46

4 COMPLIANCE MINIMIZATION USING B-SPLINE ELEMENTS 48

Objective Function 49
Sensitivity Analysis 50
Results 52
L-Shaped Structure 52
Cantilever Plate 56
Bracket Design 58
Michell Type Structure 60

Rocker Arm Design 61

5 COMPLIANT MECHANISM DESIGN 63

Introduction 63
Design Objectives Studied 67
Objective Function 69
Sensitivity Analysis 69
Results 71
Gripper Mechanism Design 71
Displacement Inverter Mechanism Design 74
Flapping Wing Mechanism 77

6 SMOOTHING SCHEME FOR MESH INDEPENDENT SOLUTIONS 80

Details of the Smoothing Scheme 82
Objective Function 82
Sensitivity Analysis 82
Results 83
Element-Type Independent Results 83
Mesh-Independent Results 85

7 CONCLUSIONS 89

Summary 89
Discussions 90
Scope of Future Work 92

LIST OF REFERENCES 94

BIOGRAPHICAL SKETCH 99

LIST OF TABLES

Table page

4-1 Compliance convergence results for the L-shaped structure..... 55

4-2 Compliance values for mesh independent results 88

LIST OF FIGURES

Figure page

1-1 Topology representation using contours of density function 15

2-1 Example of a sizing optimization problem 20

2-2 Example of a shape optimization problem 21

2-3 Example of a topology optimization problem 24

2-4 A unit cell of a microstructure with a rectangular void 28

2-5 An example of density-Young's modulus relationship (quadratic) 30

2-6 Checkerboard pattern in a half-MBB beam using SIMP approach 31

3-1 Comparison between the Von-Mises stress plots for a cantilever plate with circular support 37

3-2 One dimensional cubic B-spline element 38

3-3 Shape functions of a one-dimensional quadratic B-spline 39

3-4 Shape functions for one dimensional cubic B-spline element 40

3-5 A two dimensional quadratic B-spline element 41

3-6 A two dimensional cubic B-spline element 42

4-1 Plane stress model of a loaded L-shaped structure with a 20 x 20 mesh 52

4-2 Topology optimization results for L-shaped structure using a 20 x 20 mesh 53

4-3 Plane stress model of a loaded L-shaped structure with a 70 x 70 mesh 54

4-4 Topology optimization results for L-shaped structure using a 70 x 70 mesh 54

4-5 Compliance convergence plot for L-shaped structure for a mesh size of 70 x 70 55

4-6 Plane stress model of a cantilever plate with a 40 x 20 mesh 56

4-7 Results from Sigmund's 99 line Matlab code for the cantilever plate 57

4-8 Topology optimization results for the cantilever beam with a shear load 57

4-9 Plane stress model of the feasible domain for a bracket design 58

4-10 Topology Optimization results for the bracket design 59
4-11 Optimal topologies for Michell-truss type structure 60
4-12 Optimal topologies for the design of a rocker arm 61
5-1 Compliant mechanism design example 64
5-2 Feasible domain for gripper mechanism design 72
5-3 Topology results for a mechanical gripper design with a 30 x 30 mesh..... 72
5-4 Topology results for a mechanical gripper design with a 50 x 50 mesh..... 73
5-5 Results from ABAQUS for the gripper mechanism 74
5-6 Feasible domain for displacement inverter design..... 75
5-7 Topology results for a displacement inverter design with a 30 x 30 mesh 75
5-8 Topology results for a displacement inverter design with a 50 x 50 mesh 76
5-9 Results from ABAQUS for the inverter mechanism 77
5-10 Feasible domain for a flapping wing mechanism 78
5-11 Topology results for the flapping mechanism 78
5-12 Results from a finite element analysis on the optimum structure for the flapping mechanism..... 79
6-1 Dependence of optimal topology on mesh refinement for a Michell-truss structure using Q4 elements..... 80
6-2 Plane stress model of a loaded L-shaped structure..... 83
6-3 Topology results of L-shaped structure with smoothing for a mesh of 20 x 20 ... 84
6-4 Topology results of L-shaped structure with smoothing for a mesh of 70 x 70 ... 85
6-5 Feasible domain for a beam with a circular hole..... 85
6-6 Topology results for the beam with circular hole using Q4 elements with a mesh size of 50 x 25..... 86
6-7 Topology results for the beam with circular hole using Q4 elements with varying mesh sizes 87

Abstract of Thesis Presented to the Graduate School
of the University of Florida in Partial Fulfillment of the
Requirements for the Degree of Master of Science

TOPOLOGY DESIGN USING B-SPLINE FINITE ELEMENTS

By

Anand Parthasarathy

May 2010

Chair: Ashok V. Kumar
Major: Mechanical Engineering

Topology optimization is an approach to find the optimal material distribution or layout within a given feasible design space. The entire geometry is treated as a variable. In past approaches, this has been achieved by treating porosity or density of elements in the finite element model as the design variables. The optimization process drives the density to zero in regions where material is not needed. When density is treated as constant within each element, the resultant density distribution is not continuous and the boundaries are therefore not smooth. In this thesis, optimum designs are represented as contours of highly smooth density functions that are interpolated or approximated using the nodal values of density. The nodal values are used as the design variables and the density varies continuously within the elements. The contours of this shape density function corresponding to a threshold value are defined as the boundaries. Thus the boundaries can be expressed as implicit equations. Use of traditional finite elements like 4-node quadrilateral elements result in bilinear interpolation within an element and hence the contours will be piece-wise linear. A shape density function which is C^0 continuous will result in optimal shapes that have C^0 continuous boundaries. In this thesis, B-spline finite elements are used for topology

optimization, where the shape density function is represented using B-spline approximations to obtain smoother shapes and topology results. Unlike traditional finite elements, B-spline finite elements yield solutions that are C^1 or C^2 continuous and hence smoother shapes can be obtained. A new smoothing scheme for eliminating mesh dependence is introduced. It involves augmenting the objective function with the square of the gradient of density as a weighted sum in the optimization problem to ensure that the final topologies are not dependent on the mesh discretization. Moving barriers optimization algorithm is used to compute the optimal values of the nodal densities. Results indicate that the B-spline elements converge to optimal shapes having smooth boundaries as compared to the traditional finite elements even with a sparse mesh. Results with the smoothing scheme also indicate that the dependence on mesh discretization and the element-type are eliminated.

CHAPTER 1
INTRODUCTION

Overview

Topology optimization can be considered as an approach that optimizes the material layout or distribution within a given design space for a given set of loading and boundary conditions. It helps us find the best conceptual design that meets the design and performance requirements. Once the conceptual design is obtained, the design can be further fine tuned for better performance and manufacturability. Topology optimization helps in reducing costly design iterations before arriving at the design with optimal material distribution. Consequently, this reduces the total design time and also reduces the cost involved in the design process. Topology optimization finds application in various industries such as aerospace, mechanical, civil and automotive industries.

In a structural analysis, the design of the structure is generally known, together with the properties of the material, support conditions and loads acting on the structure. For the given set of loads, a set of equilibrium equations, constitutive equations, compatibility equations along with the boundary conditions are used to solve for the structural response such as displacements, stresses, strains etc. Conventional design process involves a series of repeated changes to the structural parameters such as the cross-sections or the shape of the structure. It is then followed by repeated structural analysis until the specific performance requirements for the structure are met. But the changes to the structural parameters are generally made by intuition or guesswork from the information obtained from the previous structural analyses. Hence the structural design obtained from such a procedure would not be an optimal one.

Structural optimization can generally be defined as a process which consists of determining the optimal values of the design variables for given design specifications. An objective function or criterion is maximized or minimized while satisfying a set of geometrical or behavioral constraints.

Sizing, shape and topology optimization are three different classes of structural optimization with different types of design variables. In sizing optimization, the design variables could be the thickness of a plate or the cross-sectional areas of a truss structure. In a shape optimization problem, the design variables describe the shape of the external boundaries of a structure or the shape of the holes in a structure. In a topology optimization problem, the entire geometry within a feasible design space is treated as the design variable.

Early topology optimization methods involved structural analysis using the finite element method, followed by removal of elements that are under-stressed to obtain an improved design. The final geometries obtained from such a method depend on the initial mesh discretization of the finite element model and hence is not reliable. Since then different methods have been used to represent the shapes in the topology optimization process. In the homogenization method, *Bendsøe and Kikuchi* [1] modeled the material as porous by assuming an underlying microstructure. The porosity of the material is treated as the design variable and the optimal distribution of the porosity of the material is to be determined. The porosity within each element in the finite element model is treated as constant. The material properties derived will then depend on the microstructure assumed and hence on the porosity of the material.

In an alternative approach called Solid Isotropic Material with Penalization (SIMP) [2], the density of each element in the finite element model is chosen as the design variable. Artificial relations between the material property and density have been used instead of assuming the material to be porous. The density within each element in the finite element model is treated as constant. The material property-density relation is generally modeled as a polynomial relation of the form,

$$E(x) = \rho(x)^p E^0 , \; p > 1 \qquad (1\text{-}1)$$

Here the density $\rho(x)$ is the design function and E^0 represents the original material properties of the given isotropic material and $E(x)$ represents the material properties as a result interpolation. Such a relation would introduce a penalty whenever the density values move away from 0 or 1. Higher the power of the density relation, lesser will be the appearance of grey areas in the final design.

Kumar and Gossard [3] also used a similar artificial material property density relation but treated the nodal values of density in the finite element model as design variables. The optimum shapes are represented as contours of highly smooth density function which are either interpolated using the nodal values of the densities. Contours of the highly smooth shape density function corresponding to a threshold value are defined as the boundaries of the geometry of the structure. This allows the representation of the boundaries using implicit equations.

An example of representation of the topology design for a short cantilever beam as contours of the density function is shown in Figure 1-2. The cantilever beam is fixed at one end and a shear load is applied to the free end of the beam. The feasible design space is the rectangular domain shown in the Figure 1-1 (a).

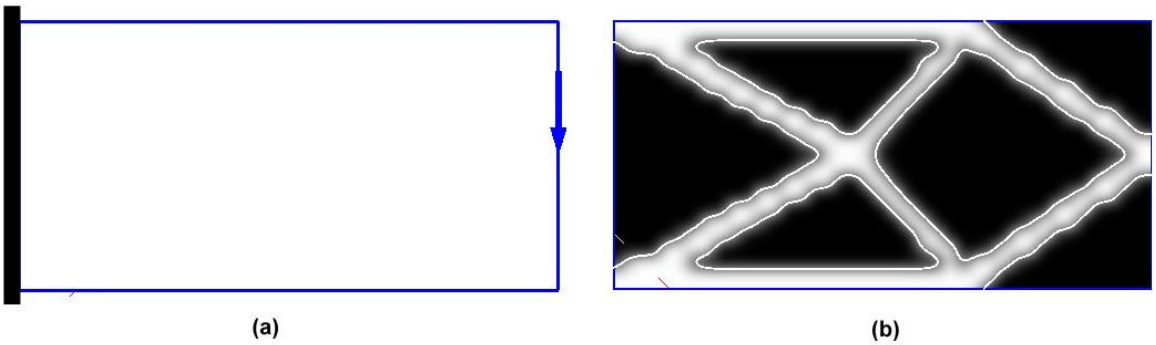

Figure 1-1 Topology representation using contours of density function A) Feasible design space with loads and boundary conditions B) Optimized lay-out for a threshold value of density = 0.5

The contour of the density function corresponding to the density value of 0.5 is defined as the boundary of the topology. It is observed that for the given support conditions and loads, the optimal lay-out turns out to be a frame-like structure as shown in the Figure 1-1 (b).

Burla and Kumar [4] implemented the B-spline finite elements for structural analysis. B-spline finite elements cannot be used with the traditional finite element method with conforming mesh due to limitations in applying boundary conditions. *Burla and Kumar* [4] used a structured grid approach called the Implicit Boundary Finite Element Method (IBFEM) to implement B-spline finite elements.

In this thesis, B-spline finite elements are used for the structural analysis for topology optimization. The contours of the shape density function which represent the boundaries of the design structure are represented using B-spline approximations. In B-spline finite elements, the displacement field in the structural analysis is also represented using B-spline approximations instead of traditional Lagrange interpolation shape functions. The use of B-spline approximations yield C^1 or C^2 continuous solutions

and therefore render smooth solutions without any shape irregularities such as the checkerboard pattern.

It has been observed that the use of either the homogenization method or the SIMP method does not yield solutions that are independent of the mesh discretization. Therefore, a new smoothing scheme is introduced here to yield solutions that are mesh-independent. The smoothing scheme filters the variations of density in the design domain and results in solutions that are independent of the mesh discretization of the finite element model. In addition to the B-spline elements inducing an inherent smoothness in the solutions, the smoothing scheme reduces the number of holes that can appear and helps achieving geometries with smooth and sharp boundaries.

The simplest type of design problem formulation to solve for an optimum topology is the design for minimum compliance. In this thesis, different examples of design of structures for minimum compliance under a constraint on the weight of the overall structure are considered. Other complex objectives such as the design of compliant mechanisms are also considered. Examples are provided to demonstrate the effectiveness of B-spline elements in representing smooth shapes particularly with a sparse mesh. Examples are also provided to demonstrate the use of the new smoothing scheme to eliminate mesh dependence of the optimal solutions. The results are compared with the results obtained using the bilinear 4-node quadrilateral elements. Results indicate that the B-spline elements result in smoother shapes and clear boundaries particularly with sparse mesh densities unlike the traditional Q4 elements.

Goals and Objectives

The goal of this research presented in this thesis is to study the use of B-spline elements for topology optimization using Implicit Boundary Finite Element Method.

The main objectives of this thesis are:

- To extend Implicit Boundary Finite Element Method for topology optimization and to use B-spline elements for various topology optimization problems.
- To study the advantage of using B-spline elements over traditional elements in obtaining smoother shapes without shape irregularities.
- To study the use of the new smoothing scheme to eliminate dependence on the initial mesh discretization of the finite element model.

Outline

The remaining portion of the thesis is organized as given below:

In Chapter 2, the past work on topology optimization as available from the literature is discussed. Various methods used to represent shapes in topology optimization such as homogenization scheme and SIMP are discussed in detail.

In Chapter 3, the theory behind the B-spline basis functions and B-spline finite elements is discussed. The details about the Implicit Boundary Finite Element method are also discussed.

In Chapter 4, design problems for minimum compliance design are considered. The objective function and the sensitivity analysis computations are also discussed. The results are compared with the results obtained using the bilinear 4-node quadrilateral elements.

In Chapter 5, the design of compliant mechanisms using topology optimization is considered. Various objective functions from the literature are discussed. The results are compared with the results obtained using the bilinear 4-node quadrilateral elements.

In Chapter 6, the implementation of the new smoothing scheme to eliminate the dependence on mesh density is discussed. Results are also shown to illustrate that the checker board pattern and other shape irregularities are eliminated.

In Chapter 7, conclusions drawn from the application of B-spline finite elements are discussed. Advantages and disadvantages of using B-spline elements over traditional finite elements are elaborated. Also, the advantages of using the smoothing scheme along with the B-spline elements are discussed. Scope of the future work is also presented.

CHAPTER 2
TOPOLOGY OPTIMIZATION

Introduction

Optimal design can be defined as being “the best feasible design according to a preselected quantitative measure of effectiveness” (*Haftka et al.* [5]). One of the most important features to be considered in the structural design process is the efficient use of materials according to the design problem under consideration. The minimum weight design was initially appreciated by the aerospace industry in which minimizing weight carries more importance than minimizing the cost of the aircrafts. Most other structural designs intend to minimize the cost of the structure although the weight of the structure indirectly affects the cost of the structure. The optimum lay-out of a structure includes information on the size, shape and the topology of the structure. Sizing, shape and topology optimization address different approaches to structural design optimization and have different types of design variables.

Sizing Optimization

In sizing optimization, the objective may be to find the optimal thickness of a plate or the optimal cross-sectional areas of the members in a truss or frame like structure. A physical quantity such as the mean compliance of the structure will then be minimized while satisfying the boundary conditions on the structure. The design variable is then the thickness of the plate or the cross-sectional area of the structural members. The main feature of the sizing optimization is that the layout or the design of the structure is known in advance. The finite element model does not change during the optimization process since the geometry change induced by changes in the design variables is minimal. Earlier work in structural optimization was mostly applied to sizing optimization

problems. More detailed information on optimal structural design and various techniques can be found in *Haftka et al.* [5] and *Kirsch* [6].

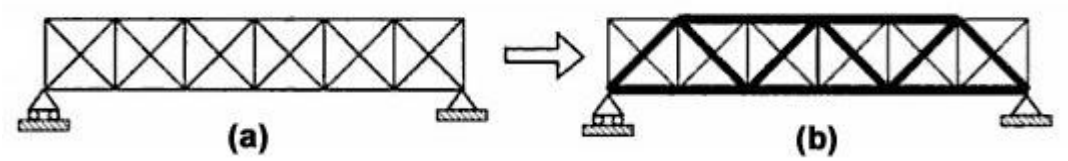

Figure 2-1 Example of a sizing optimization problem. (a) Design problem (b) Optimal solution

An example of a sizing optimization problem is shown in Figure 2-1. The design of the structure is already know a priori and the optimum cross-sectional areas of the truss or frame-like members have to be determined for the given loading and support conditions to minimize the overall weight of the structure. Some of the cross-sectional areas in the example above are increased from the initial design.

Shape Optimization

In a shape optimization problem, the objective is to find the optimum shape of the design domain by varying the boundaries of the structure or the boundaries of the holes in the structure. The design variables in a shape optimization problem describe the shape of the external boundaries of the structure or the shape of the holes in the structure. Thus the shape optimization problem is defined on a domain which itself is now treated as the design variable. As a result, the shape optimization problem requires the finite element model to change during the optimization process. Since the shape of the boundaries or the holes are continuously changing during the optimization process, careful consideration has to be paid in selecting the design variables, in maintaining the accuracy of the finite element analysis due to continuous change in the finite element

model, to improve the accuracy of the sensitivity analysis and to impose the constraints accurately due to a continuous change in the finite element mesh.

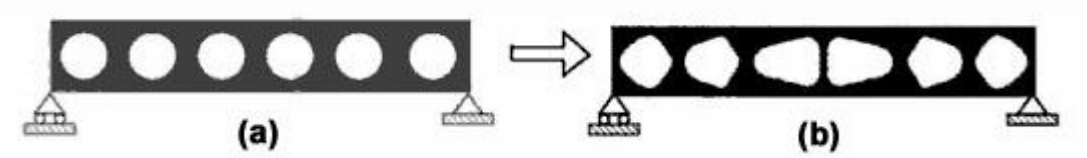

Figure 2-2 Example of a shape optimization problem. (a) Design problem (b) Optimal solution

An example of a shape optimization problem is shown in Figure 2-2. The design domain itself is changed during the optimization process to obtain the optimum design. The objective is to find the optimum boundaries of the holes in a structure or the boundaries of the structure itself to minimize the weight for a given loading and support conditions. In the example above, a design domain with pre-existing holes is to be optimized. In a shape optimization problem, the number of holes is already known and does not change during the optimization. The optimum design is shown in Figure 2-2 (b). A typical application of shape optimization would be to reduce the stress concentration around the holes in the structure. The sizing optimization would only increase or decrease the thickness of the material near the holes. On the other hand, shape optimization changes the shape of the holes to reduce the stress concentration.

Yunliang [7] reviews various numerical and analytical methods for shape optimization of structures. Various steps in the shape optimization process such as the definition of the analysis model, objective functions, design variables, representation of the boundaries of the analysis domain, finite element mesh generation and refinement, sensitivity analysis and solution methods are reviewed in detail. *Zienkiewicz and Campbell* [8] were one of the first to study the optimization of the shape of the

structures. They proposed the idea of using the nodal coordinates of the finite element mesh as the design variables in the shape optimization process [9], [10].

The representation of the shapes is the critical element in the shape optimization process. The shape variables or the design variables have to be chosen carefully to ensure that the shapes are represented accurately during the shape optimization process. There were various methods used for shape representation namely, boundary nodes for shape representation, polynomial representation of the boundary shapes and spline representation of the boundaries. These methods are explained in detail in *Yunliang* [7] and *Haftka and Grandhi* [11].

Yunliang [7] and *Haftka and Grandhi* [11] also explain in detail about the finite element mesh refinement techniques, sensitivity analysis of the finite element model, and different solution methods required for shape optimization problems. Shape optimization problems require continuous change in the finite element mesh and hence the finite element mesh refinement is a critical factor in the optimization process. Often manual mesh refinement is not a feasible solution, since the design engineer has to come up with a meshing scheme without an idea of the final optimum shape. Adaptive mesh refinement in the automated mesh generation scheme aids in resolving the problem. Mesh refinement can either be performed by increasing the number of elements or by increasing the order of the elements.

Haftka and Grandhi [11] discuss the sensitivity analysis of the objective function and constraints with respect to the design variables. There are two basic methods that can be used to compute the derivatives namely, differentiation of the finite element model and differentiation of continuum equations. Differentiation of the finite element

model can be computed using finite differences. But the method is computationally costly when the number of design variables is large. Other alternative approaches namely direct and adjoint methods can also be used. In the direct method, the derivatives of the displacement vector with respect to the design variables are computed by solving the equation obtained by differentiating the finite element equation $KU = F$ with respect to the design variables x,

$$K\frac{\partial U}{\partial x} = \frac{\partial F}{\partial x} - U\frac{\partial K}{\partial x} \tag{2-1}$$

Here *K* is the stiffness matrix, *U* is the displacement vector and *F* is the load vector.

On the other hand, the adjoint method is used to compute the derivatives of the constraints with respect to the design variables. The disadvantage of using the direct method is that the derivative of the stiffness matrix $\partial K/\partial x$ can often become costly, since the finite element mesh can change even for small changes in the boundary. Also, the distortion of the boundary elements due to the change in the mesh can lead to reduced accuracy.

One of the other methods to compute the sensitivity analysis is the continuum derivative approach. Continuum derivatives are obtained by differentiating the continuum equations with respect to the design variables. The mesh discretization is performed later and hence errors due to distortion of elements are eliminated. *Haftka and Grandhi* [11] also discuss various solution techniques used for the shape optimization process.

Shape optimization methods have various limitations in obtaining optimal shapes of the structures. The shape optimization process requires frequent changes in the finite element mesh and the accuracy of the finite element mesh can directly affect the

results. Another serious limitation in the shape optimization process is that the topology of the optimum shape is not known a priori. The boundaries of the structure are represented based on some assumptions by the design engineer at the beginning of the optimization process. Consequently it results in a restricted set of optimal solutions and that the final optimal design is topologically same as the initial ones assumed by the designer. The difficulty of changing the topology of the shapes during the optimization process increases the difficulty of the shape optimization problem.

Topology Optimization

The optimal shapes obtained using the shape optimization process is largely dependent on the initial topology. The purpose of topology optimization is to find the optimal layout of the structure within a specified feasible design domain. Therefore in topology optimization, the entire geometry within the design domain is treated as the design variable. The known quantities in the design are the loads, the support conditions and the mass of the structure to be constructed. The shape and topology of the structure are unknown quantities. The feasible design domain is defined as the space within which the optimum structure has to fit. Usually, a constraint on the mass of the structure is specified apart from the loads and the support conditions.

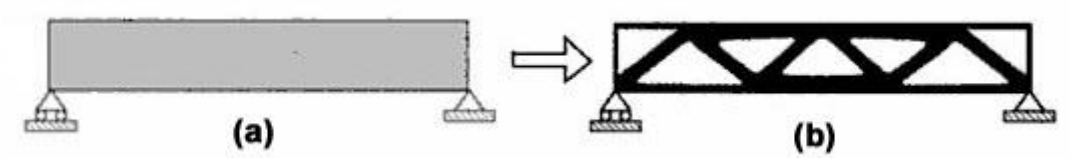

Figure 2-3 Example of a topology optimization problem. (a) Design problem (b) Optimal solution

An example of a topology optimization problem is shown in the Figure 2-3. The feasible domain is the rectangular section and the domain is discretized using a finite

element mesh. The optimal design obtained is a frame like structure with varying cross-sectional areas. An important advantage of using topology optimization over the sizing and shape optimization is the optimal geometry is not influenced by the initial guess provided by the designer.

Topology Optimization Methods

Various methods are used to represent shapes in topology optimization. The design variables are no longer the polynomial representation of the boundaries or the boundary nodal coordinates in the finite element model. Homogenization method is one of the early methods used in the topology optimization process. Materials are modeled as being porous by assuming an underlying microstructure. The relation between elastic properties and porosity are derived using the homogenization method based on the microstructure assumed. Element porosity values in the finite element model are treated as design variables and the porosity within each element is assumed to be constant. Another popular method used in topology optimization is the Solid Isotropic Material with Penalization (SIMP) method. In this method artificial material property-density relations are used. Element density values are treated as design variables and the density within each element is treated as constant.

Genetic algorithm [12]-[15] is another method used in structural topology optimization. Each design in the design space is represented as a character string and is analogous to a chromosome. Each character in a string is analogous to a gene in the chromosome. For example, the design domain can be discretized using rectangular elements, where each element represents either material or void. Each element in the finite element model can thus assume values of either 1 or 0 equivalent to material or void regions. Therefore, a string of ‘0’ and ‘1’ could be used as a chromosome to

represent a design where the number of characters is equal to the number of elements in the domain. When parent designs, chosen from the best set of designs in a generation, are grouped in pairs, two child designs per pair are created. Random mutations are performed on the genes of individual designs to make sure that two designs are not identical in a given generation. A fitness criterion is used to discard the designs in a generation based on some objective criteria. A new generation of designs is then created and the process continues iteratively until optimal designs are obtained.

Evolutionary Structural Optimization (ESO) [16]-[19] is another method used in topology optimization. It is based on the concept of gradually removing material to obtain the optimal topology. The design domain is discretized using standard finite elements and the finite element model does not change during the optimization process. The elements that have least contribution towards an objective criterion are gradually removed and the process is performed iteratively until specific performance requirement is obtained.

Level Set method [20]-[22] is a method similar to boundary variation method for shape optimization with the capability of handling topological changes. The structure to be optimized is represented by an implicit moving boundary. The moving boundary is described as a level set of a scalar function called the level set function. The structural optimization can be performed by allowing the level set function to dynamically change with time. *Wang et al.* [20] formulate the dynamic model as,

$$S(t) = \{ x(t) : \Phi(x(t), t) = k \} \tag{2-2}$$

Here Φ is the level set function corresponding to a contour value of k and x is the set of points on the boundary of the structure represented by the level set function Φ.

By differentiating this equation with time, we get

$$\frac{\partial \Phi(x,t)}{\partial t} + \nabla \Phi(x,t) \frac{dx}{dt} = 0 \qquad (2\text{-}3)$$

Here $\frac{dx}{dt}$ is the speed vector that defines the movement of the set of points x as described by the objective function to be optimized. Then, the optimal structural boundary obtained by solving the above partial differential equation.

The homogenization method and the SIMP method are discussed in detail in the following sections as the method used in this thesis is closely related to these two representations.

Homogenization Method

A study on some of the sizing and shape optimization problems, particularly plate problems, resulted in problem formulations comprising of microstructures. *Cheng and Olhoff* [23], [24] clearly demonstrated that infinite number of thin stiffener-like formations appear in the solutions of the optimization of thickness distribution of elastic plates This work led to more research on optimization problems in which the feasible set of solutions consist of regions of solid and voids. *Kohn and Strang* [25] established the idea of homogenization for the design of torsion bars which yielded three types of regions namely, solid, empty and porous, where the porous regions comprise of some material with cavities.

Bendsøe and Kikuchi [1] developed this idea further for generating optimal structural topologies. The material is defined as porous by assuming an underlying microstructure with holes. The design domain is assumed to consist of periodic repetition of the microstructure. The relation between the material property and the

porosity is derived using the homogenization method by assuming different hole sizes for the microstructure. Usually the material properties are derived for a small number of different hole sizes and then interpolated to obtain the material properties-porosity relationship. The design domain is discretized using a finite element mesh and the element porosity values are treated as design variables. The porosity within each element is treated as constant. An optimization algorithm is then used to solve for optimal distribution of porosity. The shape optimization problem is transformed into material distribution problems by use of composite materials for defining shapes in terms of porosity. An important feature of the homogenization method is that variation in the macroscopic behavior of the material is determined due to the changes in the microstructure constituents. *Bendsøe and Kikuchi* [1] have used a microstructure with square or rectangular void within a unit cell. The optimization algorithm varies the porosity in such a way that the porosity is increased for the elements where material is under-utilized and decreased where the material is highly utilized.

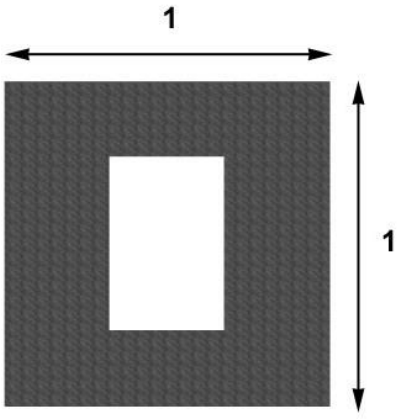

Figure 2-4 A unit cell of a microstructure with a rectangular void

An example of a unit cell with rectangular void of a microstructure is shown in Figure 2-4. The material property is thus a continuous function of the porosity and can

be determined using the homogenization method. This method thus allows you to predict the topology of the structural shapes but yields non-smooth boundaries. Hence, this method is the first step in a two-step design procedure; the second step consists of the traditional shape optimization by boundary variation method based on the shapes obtained from the first step.

Solid Isotropic Material with Penalization

The geometry of the structure obtained using the homogenization method is dependent on the microstructure assumed and the boundaries of the geometry are uneven when the mesh discretization is sparse. Checkerboard patterns are often observed when the mesh discretization used is sparse.

Bendsøe [26] suggested an idea of using artificial relations between the material property and density to represent shapes in topology optimization. The density of the elements in the finite element mesh is chosen as the design variable and is treated as constant within an element. *Kumar and Gossard* [3] introduced a similar artificial material property-density relation. The nodal values of density in the finite element mesh are treated as design variables and the density is interpolated within the elements using the nodal values. *Rozvany et al.* [27], *Yang and Chuang*.[28] used a similar approach with constant element densities. The idea of using artificial material property-density has since been called Solid Isotropic Material with Penalization (SIMP) [2]. The relationship between the density and the material properties is expressed as an empirical relationship as given below,

$$E(x) = \rho(x)^p E^0 \,,\; p > 1$$

$$\int_{\Omega} \rho(x)\; d\Omega \le V \,;\; 0 \le \rho(x) \le 1,\; x \in \Omega \tag{2-4}$$

Here the density $\rho(x)$ is the design variable and E^0 represents the original material properties of the given isotropic material and *E(x)* represents the material properties as a function of density. As the name suggests, the SIMP method penalizes the intermediate values of density between 0 and 1, since the stiffness obtained for the intermediate values is extremely small when compared to the volume of the material used. In general, a value of p > 1 is desired to drive the values of density towards 0 or 1. In other words, by specifying a higher value of *p* makes it becomes uneconomical to have intermediate densities in the optimal design. A simple plot between the density and the Young's modulus of the material for a quadratic relationship is shown in Figure 2-5.

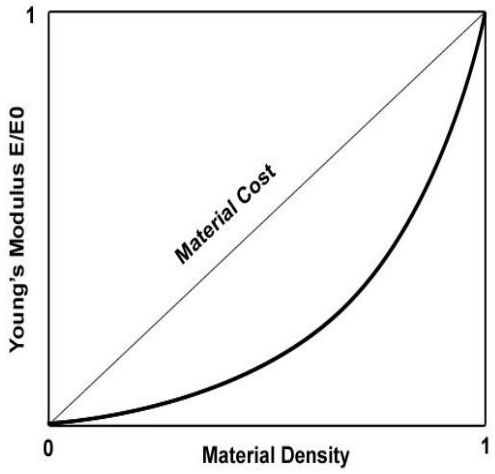

Figure 2-5 An example of density-Young's modulus relationship (quadratic)

One of the main issues that significantly influence the computational results obtained with the layout optimization problems is the appearance of checkerboard patterns. The checkerboard pattern refers to the variation of the density in a periodic fashion similar to a checkerboard consisting of solid and void regions. It can be attributed to the discretization of the original continuous design domain. *Jog and Haber*

[29] state that the origin of the checkerboard pattern is related to the numerical instabilities that exist in the finite element approximations in a distributed-parameter optimization such as the density or porosity distribution problems and the checkerboard pattern is not associated with any specific material model. *Jog et al.* [30] suggest that the abnormal behavior of the solutions to topology optimization problems is due to the mixed finite element models, involving different displacement and density fields.

Diaz and Sigmund [31] suggest that the checkerboard patterns are due to the numerical instability in the finite element model and that the finite element discretization make the checkerboard patterns appear more efficient by overestimating the stiffness of the checkerboards. In the standard compliance minimization problems, the mean compliance is minimized or the strain energy density is maximized with a constraint on the allowable material. With the density or porosity being constant within each element, the finite element approximation favors the arrangement of the material in a checkerboard fashion so that the strain energy is maximized. Results have shown that both the bilinear and quadratic quadrilateral elements result in checkerboard patterns in both the homogenization and SIMP approaches.

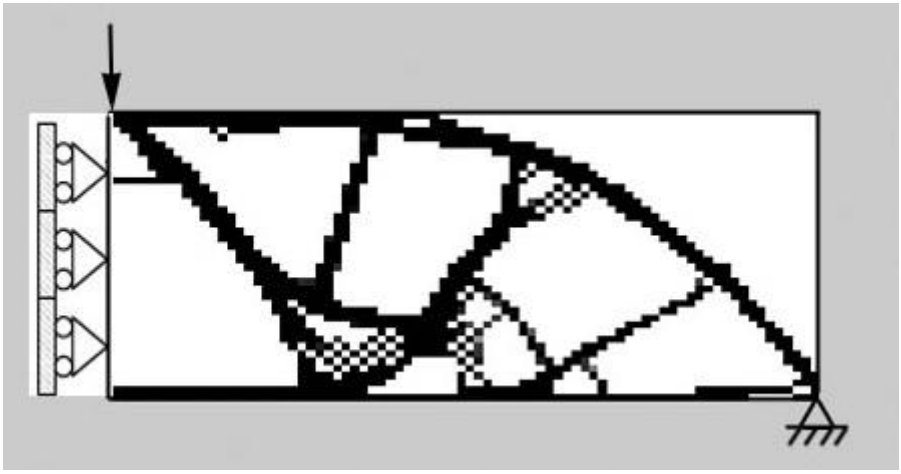

Figure 2-6 Checkerboard pattern in a half-MBB beam using SIMP approach

Figure 2-6 shows a half-MBB beam example with the boundary conditions and loads. The results have been obtained using the code from *Sigmund* [32] with *80 x 40* quadrilateral elements. Checkerboard patterns are evidently visible in the final optimal solution.

The approach developed by *Kumar and Gossard* [33] in which the boundaries of the structure are represented using contours of the shape density function has been used in this thesis. In this method, the nodal values of densities in the finite element discretization are the design variables and the densities within each element are not treated as a constant. Instead, the nodal values of the densities are interpolated within each element using the shape functions for the element. Since the contours of the density function corresponding to a threshold value are used to represent the boundaries, a new internal boundary will be created wherever the value of the density function reaches the threshold value.

Similar to different microstructure assumptions leading to different material property-porosity relations in the homogenization method, different assumptions on the variations of elastic modulus with density lead to different material property relations. The material inside the shape should be fully dense $(\phi = 1)$ and the material should have lowest possible density where holes are located. At the boundaries, the density would be desired to transition sharply from the highest value to the lowest threshold value, so that we have clear and well defined boundaries. Higher order approximations of material property-density relations lead to clear and well-defined boundaries.

The stress-strain relationship for a two dimensional plane stress case may be given as,

$$\{\sigma\} = [D(\phi)]\{\varepsilon\} \tag{2-5}$$

$$[D(\phi)] = \begin{bmatrix} d_{11} & d_{12} & 0 \\ d_{12} & d_{22} & 0 \\ 0 & 0 & d_{33} \end{bmatrix} \tag{2-6}$$

$[D(\phi)]$ is the elasticity matrix which is a function of the density. Assuming that the Young's modulus *E* varies as p^{th} power of the density function, the relations for the elasticity coefficients as a function of the density ϕ can be given as,

$$d_{11} = \frac{E\phi^p}{1-\nu^2} \tag{2-7}$$

$$d_{22} = \frac{E\nu\phi^p}{1-\nu^2} \tag{2-8}$$

$$d_{33} = \frac{E\phi^p}{2(1+\nu)} \tag{2-9}$$

In the above assumption, Poisson's ratio ν is not a function of the density function. Therefore, the elastic coefficients reduce to zero only when the value of the density ϕ becomes zero, *i.e.*, $d_{ij} = 0$ for $\phi = 0$. The elasticity matrix can then be defined as,

$$[D_p(\phi)] = [D]\phi^p \tag{2-10}$$

Here $[D]$ is the elasticity matrix for a plane stress or plane strain problem.

The use of traditional finite elements such as bilinear 4-node quadrilateral elements in the structural analysis for topology optimization can only yield C^0 continuous solutions. The resulting shapes are generally not smooth and well connected unless a dense mesh discretization is used. Therefore, B-spline elements are used for topology optimization to obtain smoother shapes in this thesis. In B-spline elements, both the displacement and the density fields are approximated using B-spline

approximations. The B-spline elements have a wider span and result in inherent smooth boundaries even with a sparse mesh discretization. They also eliminate the appearance of the checkerboard patterns. B-spline elements are discussed in detail in the following chapter.

CHAPTER 3
B-SPLINE FINITE ELEMENTS

Introduction

B-spline functions are smooth polynomial functions which can be used for approximation of a given set of points. Lagrange interpolation functions used in traditional FEM are C^0 continuous irrespective of the basis used. B-spline basis functions can provide with higher degree of continuity depending on the degree of the polynomial used. For example, quadratic B-splines can provide solutions that are C^1 continuous throughout the domain and cubic B-splines can provide us solutions that are C^2 continuous. The summation of the B-spline basis functions adds up to unity and this property, called the partition of unity, is an important property for convergence of the approximate solutions. Gauss quadrature can be used to integrate the B-spline basis functions since they are simple polynomials.

B-spline approximation is not being used in traditional finite element method because they do not satisfy Kronecker-delta property and hence Dirichlet boundary conditions are difficult to apply. *Kumar et al.* [34] introduced the Implicit Boundary Finite Element Method (IBFEM) where they use specially constructed solution structures to impose boundary conditions. In IBFEM, a structured mesh is used for the analysis and the boundaries of the geometry are represented accurately using equations. The advantages of using a structured grid approach is that they are easier to generate and all the elements in the domain are regular and undistorted.

B-splines can be classified into three types namely uniform, non-uniform and NURBS. Uniform B-splines have equally spaced nodes in the parametric space. Non-uniform B-splines need not have equally spaced nodes in the parametric space.

NURBS uses rational basis functions and are a generalized form of the non-uniform B-splines. *Burla and Kumar* [4] used uniform B-splines to construct solutions over a structured mesh. Boundary conditions are difficult to apply when B-spline approximations are used to represent the solution because the value of the approximation at the nodes is not equal to the nodal value. A summary of B-spline finite elements and methods used in IBFEM to impose Dirichlet boundary conditions are discussed in the following sections.

B-spline Elements

B-spline approximations were originally used in applications related to geometric modeling to represent smooth curves. Traditional finite element methods use Lagrange interpolation functions which typically result in C^0 continuous solutions between adjacent elements. C^0 continuous solutions have discontinuities in representing stresses and strains across the boundaries of the adjacent elements. Hence, smoothing schemes are required to plot these quantities such that they appear continuous with the analysis domain. B-spline basis functions provide higher degree of continuity depending on the degree of polynomial used. Therefore, when B-spline basis functions are used in structural analysis, they yield stresses and strains that are continuous between elements and hence no separate smoothing scheme is required to represent the solutions. B-spline finite elements were introduced by *Burla and Kumar* [4] to be used in structural analysis using IBFEM.

An example of von-mises stress plot to demonstrate the continuity between elements is shown in Figure 3-1. Let us consider a cantilever plate of size 0.5 x 0.4 with a circular support and end loading of 10000 N. The material of the beam is assumed to

be steel with Young's modulus equal to 200 GPa and Poisson's ratio of 0.3. The domain is discretized with 20 x 20 elements as shown in Figure 3-1 (a).

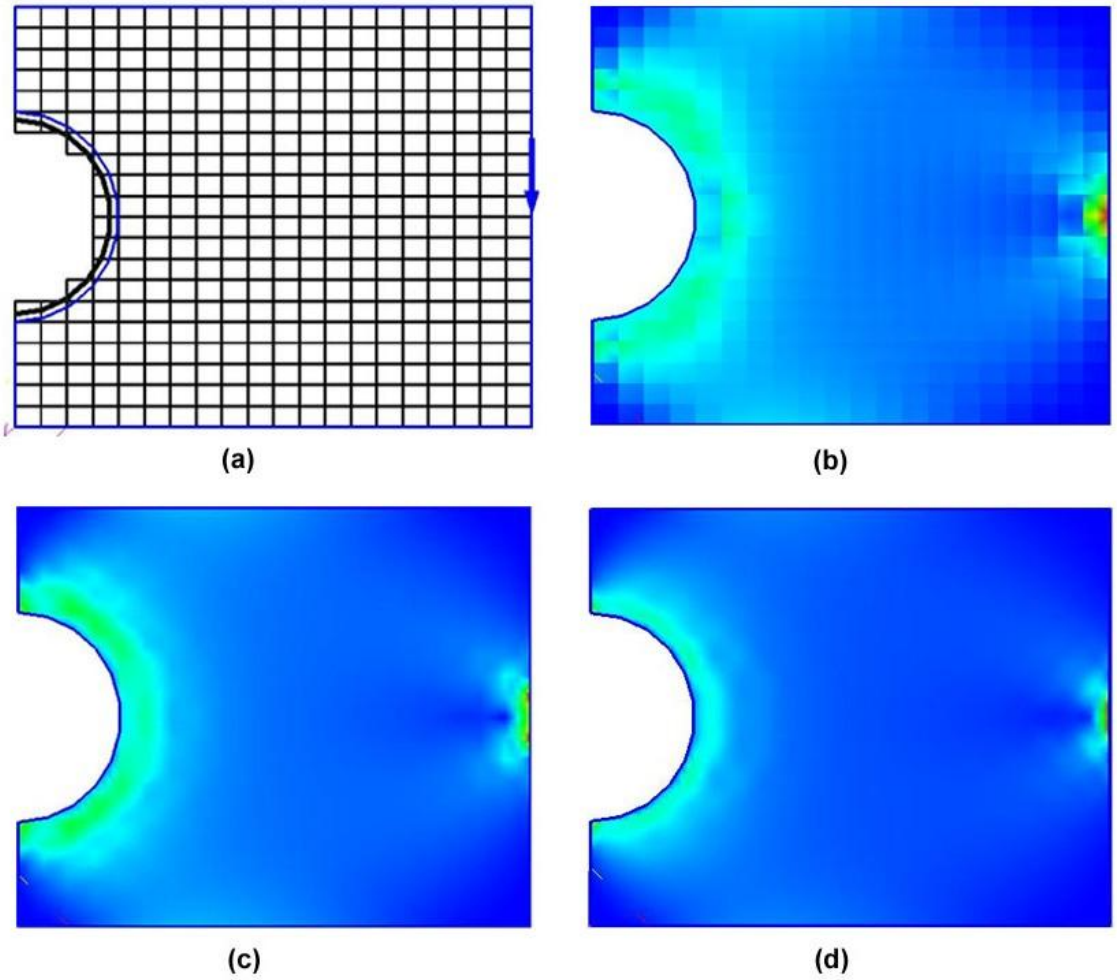

Figure 3-1 Comparison between the Von-Mises stress plots for a cantilever plate with circular support. (a) Applied loads and boundary conditions with mesh discretization (b) Quad 4 node elements (c) B-spline 9 node elements (d) B-spline 16 node elements

The plots of Von-Mises stress for the quadratic B-spline 9 node and cubic B-spline 16 node elements are shown in Figure 3-1 (c) and d) and the results are compared with the traditional Quad 4 noded elements shown in Figure 3-1 (b). It is evident from the plots that the stress distribution in the Q4 elements is discontinuous while the stress distribution in the B-spline elements is continuous.

The nodes of a B-spline finite element are called the support nodes. *Burla and Kumar* [4] used a polynomial definition for B-splines in the implementation of B-spline finite elements in IBFEM instead of a recursive definition. B-spline elements have an independent parameter space for each element in the grid which varies from [-1,1] as in the traditional iso-parametric finite elements.

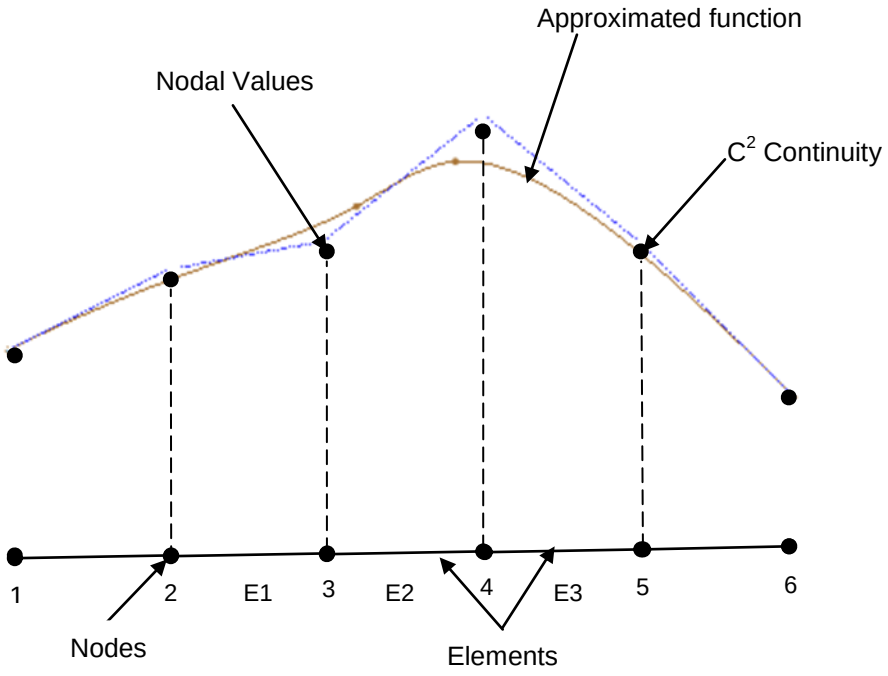

Figure 3-2 One dimensional cubic B-spline element

An example of a one dimensional cubic B-spline which is C^2 continuous is illustrated in Figure 3-2. It can be observed that, unlike the traditional finite element interpolation, the B-spline approximation does not pass through the nodal values. For example, the element E2 is defined between the vertex nodes 3 and 4 but the B-spline approximation defined over E2 (referred to as its span) is controlled by four nodes (2-5). These nodes are referred to as the support nodes. The B-spline approximation does not

pass through the nodal values at each support node unlike the traditional interpolation functions. Hence, the displacement at a given support node is not equal to the actual displacement at that node and applying an essential boundary condition at that node is not equivalent to assigning a desired value to that node.

Burla and Kumar [4] derived the polynomial expressions for the B-spline basis functions using the continuity requirements between adjacent elements. The continuity requirements along with the partition of unity property are used to derive the B-spline basis functions. The basis functions for the quadratic B-spline element can thus be derived as,

$$N_1 = \frac{1}{8}(1-2r+r^2) \tag{3-1}$$

$$N_2 = \frac{1}{8}(6-2r^2) \tag{3-2}$$

$$N_3 = \frac{1}{8}(1+2r+r^2) \tag{3-3}$$

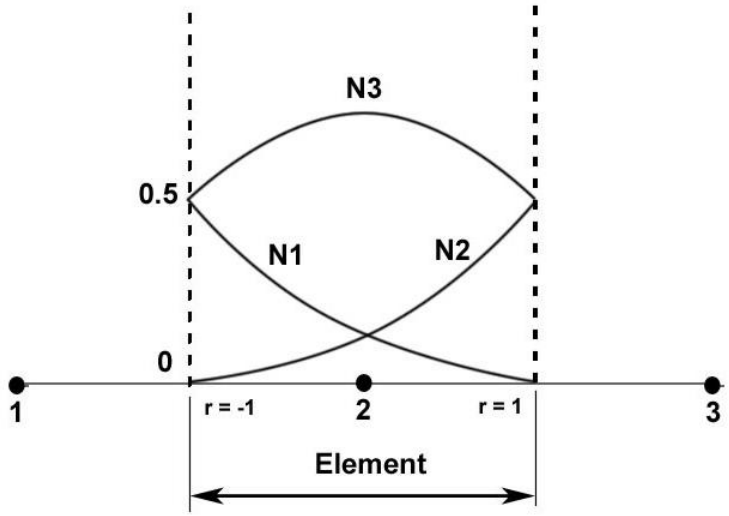

Figure 3-3 Shape functions of a one-dimensional quadratic B-spline

The plot of the shape functions for a quadratic B-spline element is shown in Figure 3-3. Since the order of the quadratic B-spline element is two, it is represented by three shape functions *N1*, *N2* and *N3*. The element has three support nodes and two of the support nodes lie outside the element in the parametric space represented between *r* = *-1* and *r* = *1*.

Again using the continuity requirements and the partition of unity, the basis functions for a cubic B-spline element can be derived as,

$$N_1 = \frac{1}{48}(1-3r+3r^2-r^3) \tag{3-4}$$

$$N_2 = \frac{1}{48}(23-15r-3r^2+3r^3) \tag{3-5}$$

$$N_3 = \frac{1}{48}(23+15r-3r^2-3r^3) \tag{3-6}$$

$$N_4 = \frac{1}{48}(1+3r+3r^2+r^3) \tag{3-7}$$

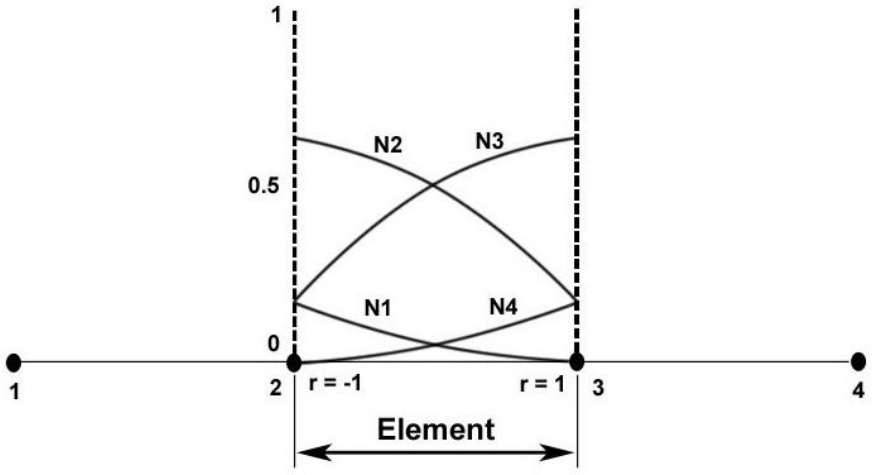

Figure 3-4 Shape functions for one dimensional cubic B-spline element

The plot of the shape functions for a cubic B-spline element is shown in Figure 3-4. The order of a cubic B-spline element is three and hence it has four support nodes and four shape functions. Two of the support nodes coincide with the nodes of the element in the parametric space.

From the plots of Figure 3-3 and Figure 3-4, it is evident that the B-spline basis functions are not unity at their corresponding nodes and do not vanish at the other nodes. Therefore, B-spline basis functions do not satisfy the Kronecker-delta property and the approximation constructed using these basis functions do not interpolate nodal values.

Burla and Kumar [4] constructed the basis functions for higher-dimensional B-spline elements by taking the product of the 1D B-spline elements. The structured grid used in IBFEM has elements that are regular quadrilaterals (square/rectangular) or regular hexahedra (cube/cuboid). Hence, the mapping from the parametric space to the real space is linear.

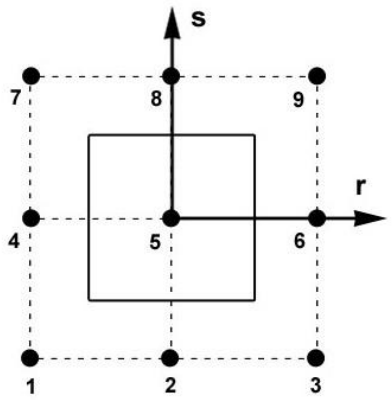

Figure 3-5 A two dimensional quadratic B-spline element

A two dimensional quadratic B-spline element is shown in Figure 3-5. The basis functions of a two-dimensional quadratic B-spline element are constructed as a product

of the basis functions of a 1D quadratic B-spline element. The span of the element is defined by nine support nodes. But none of them are at the vertices of the element in the parameter space defined by the square $[-1,1]\times[-1,1]$. Some of the support nodes lie outside the element and are shared by the neighboring elements. A 2D bi-quadratic B-spline element has 9 basis functions, where as a 3D bi-quadratic B-spline element has 27 basis functions. The shape functions for a 2D quadratic and a 3D quadratic B-spline element can be expressed as,

$$\begin{aligned} N^{2D}_{3(j-1)+i}(r,s) &= N_i(r)N_j(s), \quad i,j=1,...,3 \\ N^{3D}_{9(k-1)+3(j-1)+i}(r,s,t) &= N_i(r)\,N_j(s)\,N_k(t), \qquad i,j,k=1,...,3 \end{aligned} \tag{3-8}$$

A two dimensional cubic B-spline element is shown in Figure 3-6. The basis functions of a two dimensional cubic B-spline element are constructed as a product of the basis functions of a 1D cubic B-spline element. The span is defined by 16 nodes and there are four nodes one at each vertex of the element defined in the parameter space define by the square $[-1,1]\times[-1,1]$. Some of the support nodes lie outside the element and are shared by the neighboring elements.

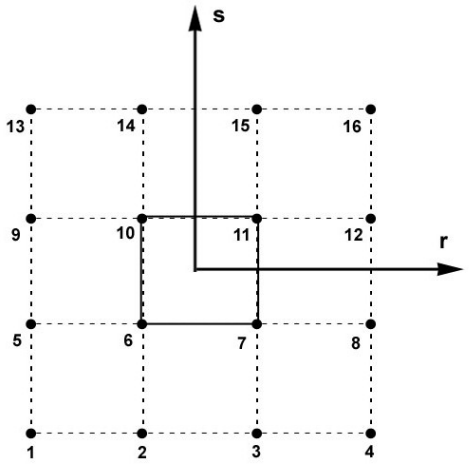

Figure 3-6 A two dimensional cubic B-spline element

A 2D bi-cubic B-spline element has 16 basis functions, where as a 3D bi-cubic B-spline element has 64 basis functions. The shape functions for a 2D cubic and a 3D cubic B-spline finite element can be expressed as,

$$N^{2D}_{4(j-1)+i}(r,s) = N_i(r)\,N_j(s), \quad i,j = 1,..,4$$
$$N^{3D}_{16(k-1)+4(j-1)+i}(r,s,t) = N_i(r)\,N_j(s)\,N_k(t), \quad i,j,k = 1,...,4 \tag{3-9}$$

Merits and Demerits of B-spline Elements

Unlike the traditional finite element shape functions, B-spline basis functions do not attain unity at their corresponding nodes and do not vanish at the other nodes. Therefore, the approximation using B-splines do not interpolate the nodal values. Since C^1 or higher continuity is obtained using B-spline basis functions, the stresses and strains are represented smoothly across the elements and no additional smoothing scheme is needed. There is thus a clear advantage of using B-spline basis functions over the traditional Lagrange interpolation functions for structural analysis. But the use of B-spline elements results in an additional overload on the computational costs due to the fact that higher order polynomials have to be evaluated in B-spline finite elements. On the other hand, since B-spline elements yield extremely smoother results when compared to the traditional finite elements, smoother results could be obtained even with far fewer elements.

Since the B-spline approximation does not interpolate the nodal values and the displacements at the nodes are not the actual displacements, applying boundary conditions is a challenge with the B-spline elements. Fixing a node of the element is not equivalent to fixing actual displacement at the node to zero. Traditional finite element methods cannot be used to use B-splines for structural analysis due to difficulties in

imposing boundary conditions. Therefore, alternate approaches such as Implicit Boundary Method [34] must be used. This method allows us to impose boundary conditions even if there are no nodes on the boundary. In this thesis, B-spline elements defined using the Implicit Boundary Method are used.

Implicit Boundary Finite Element Method

In the traditional finite element method, a conforming mesh is used to discretize the analysis domain or geometry. Conforming mesh generation algorithms can be unreliable for complex geometries. They often result in distorted elements along the boundary of the analysis domain which can induce large errors in the solution. Also, the cost of mesh generation is generally too high. Several alternative methods exist and they can be broadly classified as meshless methods and non-conforming mesh or structured grid approach.

In this thesis, Implicit Boundary Finite Element Method (IBFEM) developed by *Kumar et al* [34] is used. IBFEM uses a structured grid approach for the analysis and uses approximate step functions as weighting functions as a solution structure to impose Dirichlet boundary conditions. This method can impose the boundary conditions even if the boundary is guaranteed to have no nodes or when the shape functions used for the structural analysis do not satisfy Kronecker-delta property.

Solution Structure

Kumar et al [34] constructed a solution structure using the implicit equations of the boundaries such that the Dirichlet boundary conditions are automatically satisfied. Let u be a trial function defined over the analysis domain Ω that must satisfy the boundary

condition $u = a$ along the boundary Γ^a. If $\Phi_a(x) = 0$ $(x \in \Omega)$ is the implicit equation of the boundary Γ^a, then the trial function can be defined as

$$u(x) = \Phi_a(x) U(x) + a(x) \tag{3-10}$$

The solution structure defined in the equation (3-10) will then definitely satisfy the boundary condition $u = a$ along the boundary Γ^a. The variable part of the solution structure $U(x)$ is replaced by a function defined by piecewise interpolation or approximation within the elements of the structured grid. In such a solution structure, the function $\Phi_a(x) = 0$ behaves like a weighting function. Since these functions are used in imposing the Dirichlet boundary conditions, these functions are called as the Dirichlet functions or *D*-functions. Instead of using the implicit equations of the boundaries itself as *D*-functions, Kumar et al. [34] uses approximate step functions constructed using the implicit equation of the boundary to define the solution structure. The advantage of using step functions is that all the internal elements can be treated as identical to each other. A trial solution structure for the displacement field such that the Dirichlet boundary conditions are satisfied is given by,

$$\{u\} = [D]\{u_g\} + \{u^a\} \tag{3-11}$$

In this solution structure, $\{u_g\}$ is a vector of grid variables or the nodal values of the grid and $\{u^a\}$ is the vector containing the boundary values specified at the essential boundaries. $[D]$ is a diagonal matrix that consists of the *D*-functions D_i as the diagonal components that vanish on the essential boundaries on which the i^{th} component of the displacements are specified. The displacements are not the variables in IBFEM and the nodal variables to be solved for are the grid variables in. No assumptions are made to

restrict the choice of shape function to be used to represent the grid variables. Kumar et al. [34] used with a variety of basis functions with IBFEM such as the Lagrange interpolation, B-spline basis functions.

Dirichlet Functions

The D-function D_i is a function that vanishes on all essential boundaries where the i^{th} component of the displacement is specified. Also, the gradients of the D-functions do not vanish at all the essential boundaries to ensure that the gradients are not constrained. Moreover, D-functions ensure that they are non-zero inside the analysis domain so that the solution is not constrained anywhere else in the domain other than the essential boundaries. Implicit equations of the boundary can be used to impose the boundary conditions using D-functions.

Kumar et al [34] used approximate step functions which can be constructed using any type of implicit function on the boundary. Let a boundary be represented using implicit equations Φ. The step function at any given point x on such a boundary where boundary condition is specified is defined as:

$$D(\Phi)=\begin{cases} 0, & \Phi \le 0 \\ 1-\left(1-\dfrac{\Phi}{\delta}\right)^k, & 0 \le \Phi \le \delta \\ 1, & \Phi \ge \delta \end{cases} \tag{3-12}$$

This function varies between 0 and 1 within a strip of narrow width δ near the boundary and then remains at unity within the analysis domain. In IBFEM, this approximate step function is used as the Heaviside step function in the limit $\delta \to 0$. Unlike in traditional approximations of step functions where it has a value of 0.5, this function has a value of zero on the boundary in the limit $\delta \to 0$. Moreover, $D(\Phi)$ to be

used as a *D*-function, the gradient of $D(\Phi)$ has to be non-zero at the essential boundaries ($\Phi = 0$). In the above expression for $D(\Phi)$, *k* is the order of the *D*-function. At $\Phi = \delta$ this function has a C^{k-1} continuity. In IBFEM, the *D*-function is used with values of $\delta \approx 10^{-5}$ or even smaller. This expression for the *D*-function can be used only when an essential boundary condition has to be applied on a single boundary Φ that passes through a boundary element. When an essential boundary condition has to be applied on multiple boundaries passing through a boundary element, the *D*-functions have to be constructed as Boolean combinations of the individual step functions.

In this thesis, topology optimization problems are studied with the Implicit Boundary Finite Element method using the B-spline approximations to obtain smoother shapes and designs and compared with the traditional finite elements.

CHAPTER 4
COMPLIANCE MINIMIZATION USING B-SPLINE ELEMENTS

Topology optimization of solid structures involves the determination of optimal material distribution within a feasible domain. In this thesis, B-spline finite elements are applied to topology optimization problems to obtain smooth shapes. The contours of the density function which define the boundaries of the structure are represented using B-spline approximations to obtain smoother shapes. The nodal values of densities in the feasible domain are treated as the design variables and the density is approximated within each element using B-spline approximations. Both the displacement field and the density field are represented using B-spline approximations. Therefore, the numerical instability due to mixed formulations in the finite element method is eliminated. Quadratic (B-spline 9N) and cubic (B-spline 16N) B-spline elements have been used in this thesis to represent topology results. The optimal shapes obtained are compared with the results obtained using 4-node bilinear quadrilateral elements (Quad 4N).

Solid Isotropic Material with Penalization (SIMP) approach is used and hence the material properties of a given isotropic material are represented as a polynomial relation of the density of the material. The density-material property relation can be expressed as,

$$E(x,y) = \phi(x,y)^p E_0, \quad p > 1 \tag{4-1}$$

Here, $\phi(x,y)$ is the density of the material at a given *(x,y)* and E_0 represents the material properties of the given isotropic material. The density interpolates the material properties between *0* and E_0. In the SIMP method, a polynomial power of $p > 1$ has to be used so that the intermediate densities are unfavorable *i.e.*, the stiffness obtained at

a specific region in the design domain will be too small when compared to the volume of the material used. In this thesis, a polynomial power of $p \geq 3$ has been used.

Initially, the nodal values of density are all set to unity so that the geometry is identical to the feasible domain. During the optimization, an objective criterion is minimized or maximized by changing the nodal values of density. The optimization problem is solved under a constraint on the mass of the structure. The constraint on mass is specified as a fraction of the initial mass of the feasible domain. The problems treated in this chapter are the design problem formulations for minimization of compliance (maximization of global stiffness) of the structure under a constraint on the mass of the structure.

Objective Function

Consider a domain $\Omega \text{ in } R^2 \text{ or } R^3$ in which the optimal design could be a possible solution. The reference domain Ω is chosen so as to allow for a definition of the applied loads and boundary conditions. An optimal choice of the stiffness tensor $E(x, y)$ has to be determined over the reference domain. For an arbitrary virtual displacement of δu, the minimum compliance design can be stated in the weak form as,

$$\text{Minimize: } L(u) = \int_{\Omega} b\,u\,d\Omega + \int_{\Gamma} t\,u\,ds \tag{4-2}$$

$$\text{such that, } \int_{\Omega} E(x, y)\,\varepsilon(u)\,\varepsilon(\delta u)\,d\Omega = \int_{\Omega} b\,\delta u\,d\Omega + \int_{\Gamma} t\,\delta u\,ds, \quad \text{for all } \delta u \in U \tag{4-3}$$

$$\text{subject to: } M(\phi) = \int_{\Omega} \phi\,d\Omega \leq M_0 \tag{4-4}$$

In the optimization problem statement above, *U* denotes a set of kinematically admissible displacement fields, *b* are the body forces and *t* are the boundary traction forces.

The optimization objective can be restated when a finite element model is used to solve for the optimum nodal densities and in turn optimum stiffness tensors. The objective function can then be stated as

$$\text{Minimize: } L(\phi) = F^T \{U\} \tag{4-5}$$

$$\text{subject to: } M(\phi) = \int_{\Omega} \phi \, d\Omega \leq M_0 \tag{4-6}$$

$$\int_{\Omega_0} \{\delta\varepsilon\}^T [D(\phi)] \{\varepsilon\} \, d\Omega = \int_{\Gamma} \{\delta u\}^T \{f\} \, d\Gamma \tag{4-7}$$

$$\phi_{th} \leq \phi \leq 1 \tag{4-8}$$

Here $\phi(x, y)$ is the density function, *F* is the applied traction load and {U} is the displacement vector. When the shape defined by the density function varies, the structural properties must vary accordingly. Consequently, the material property coefficients defined in the $[D]$ matrix must depend on the density function $\phi(x, y)$. The material property-density relation should be such that when the density decreases in a region, the stiffness of the structure should decrease accordingly causing the material to become more compliant in that region.

Each evaluation of the objective function requires a finite element analysis to compute the displacement at the nodes of the finite element mesh. Therefore, an algorithm that does not require excessive number of objective function evaluation is preferred. In this thesis, a modified form of sequential linear programming called the Moving Barriers algorithm [35] has been used.

Sensitivity Analysis

The density-material property relation should be defined such that if the density is decreased in a region, the stiffness should decrease correspondingly causing the

material to become weaker in that region. This could be achieved if the gradient of the objective function with respect to the design variables, $\frac{\partial L(\phi)}{\partial \phi_i}$ is negative. The optimization algorithm would therefore decrease the densities in those regions where the material in underutilized resulting in new holes to be created or shrinking of existing boundaries inwards. Sensitivity analysis is defined as the method of computing the gradient of the objective function and the constraints with respect to the design variables. A gradient based optimization algorithm would require the evaluation of the gradients to find the direction of moving towards the optimal solution. The gradient of the objective function is given by,

$$\frac{\partial L(\phi)}{\partial \phi_i} = F^T \frac{\partial \{U(\phi)\}}{\partial \phi_i} \tag{4-9}$$

The gradient of the nodal displacements can be computed by the standard design sensitivity analysis methods. The equilibrium equations are reduced to a set of linear simultaneous equations in a finite element model which is given by,

$$[K]\{U\} = \{F\} \tag{4-10}$$

$[K]$ is the stiffness tensor, $\{U\}$ contains the nodal displacements u_i and $\{F\}$ is the load vector. The gradient of u_i can be computed by solving the equation,

$$[K]\frac{\partial \{U\}}{\partial \phi} = \lambda \tag{4-11}$$

Here λ is the adjoint variable that can be computed as,

$$\lambda = -\frac{\partial [K]}{\partial \phi}\{U\} \tag{4-12}$$

Results

L-Shaped Structure

The topology optimization of a L-shaped feasible domain for minimum compliance with a constraint on the weight of the structure is performed. The L-shape feasible domain was modeled with B-spline 9 node and 16 node elements and the optimization of the material distribution of the structure for minimum weight design was performed. The results are compared with the traditional 4-node quadrilateral elements.

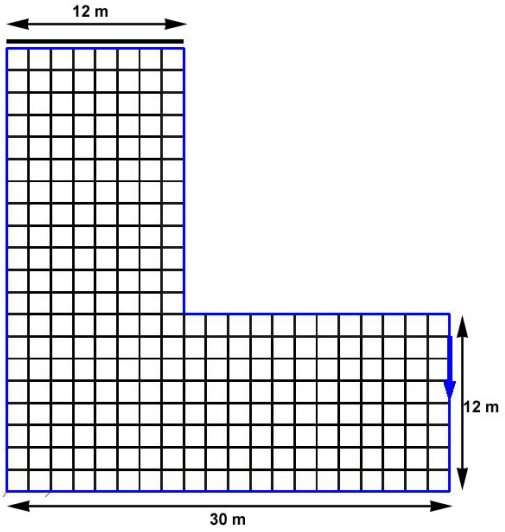

Figure 4-1 Plane stress model of a loaded L-shaped structure with a 20 x 20 mesh

The plane stress model of the L-shaped region with the dimensions and the mesh discretization for the design problem is shown in Figure 4-1. A shear load of 200 N is applied along the right edge and the domain is constrained along the top edge. The material of the domain is assumed to be steel with modulus of elasticity equal to 200 GPa and the Poisson's ratio of 0.3. The original domain has been discretized with a sparse mesh of 20 x 20 elements.

The topology results of the optimal designs are shown in Figure 4-2. The topology designs are obtained using bi-linear 4 node quad, B-spline 9 node and B-spline 16 node

elements. SIMP interpolation method with the penalty parameter $p = 4$ for the density function and the allowable material volume fraction of 0.5 is used.

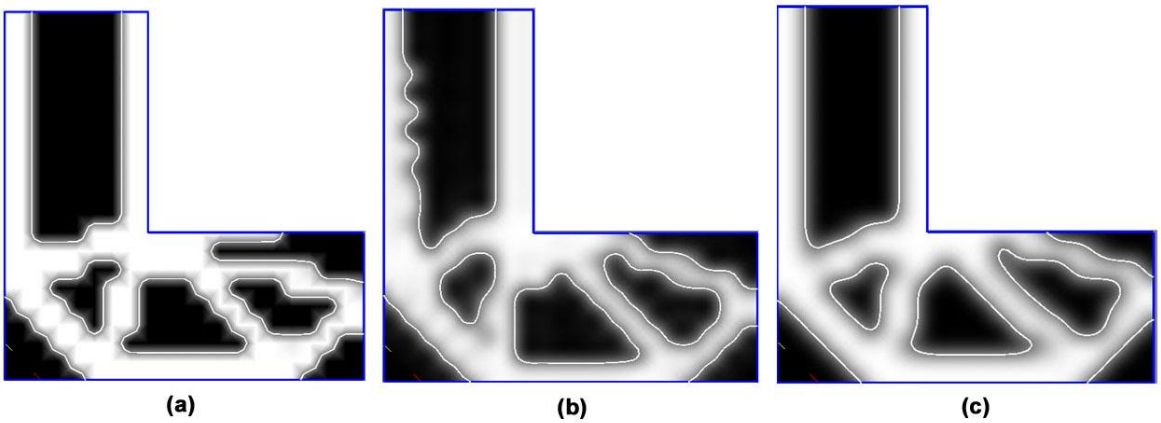

Figure 4-2 Topology optimization results for L-shaped structure using a 20 x 20 mesh and volume fraction of 0.5 (a) Quad 4N element (b) B-spline 9N element (c) B-spline 16N element

It can be observed that the use of B-spline finite elements resulted in considerably smoother shapes even with fewer elements when compared with the bi-linear 4-node quad elements. It can be observed that with the use of sparse mesh, quadrilateral elements result in a geometry that has steps along the boundary. The optimal geometries obtained using B-spline elements are smoother and have fewer holes with the boundaries represented using 16 node elements having absolutely no wriggles.

The second part of this example demonstrates the role of mesh discretization on the solutions obtained. A much more refined mesh discretization was used to check if the topologies obtained would be any different from the topologies obtained using a sparse mesh. A refined mesh discretization of 70 x 70 elements is then applied to the L-shaped region. A penalty parameter of $p = 4$ for the density function and the allowable material volume fraction of 0.5 was used. The mesh discretization for the design problem is shown in Figure 4-3.

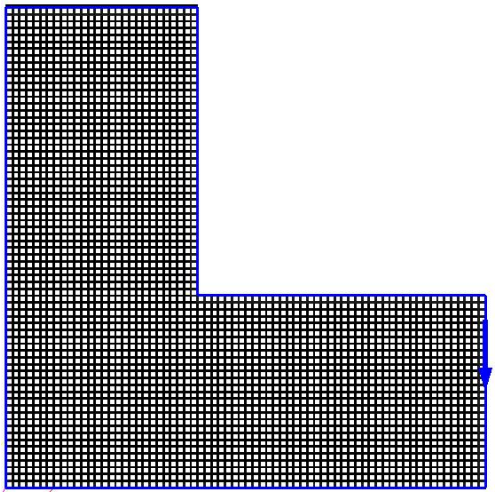

Figure 4-3 Plane stress model of a loaded L-shaped structure with a 70 x 70 mesh

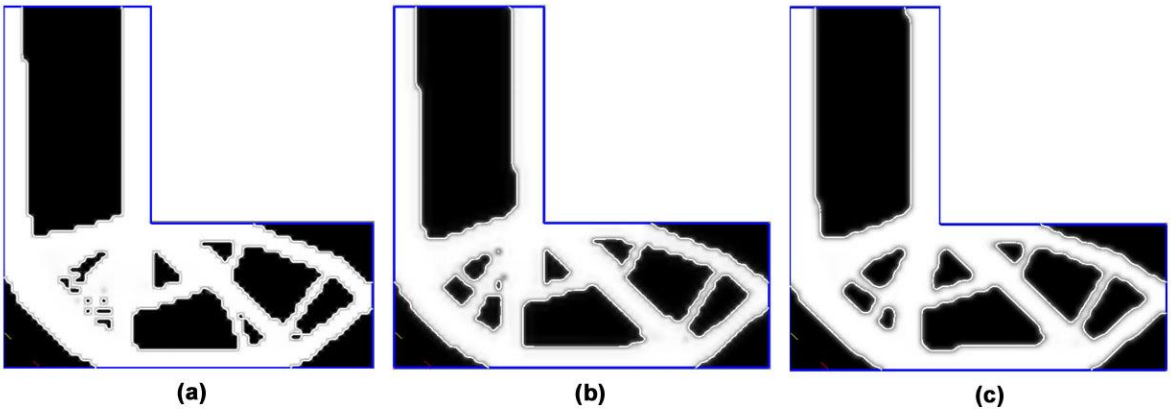

Figure 4-4 Topology optimization results for L-shaped structure using a 70 x 70 mesh and volume fraction of 0.5 (a) Quad 4N element (b) B-spline 9N element (c) B-spline 16N element

The topology results with a refined mesh are shown in Figure 4-4. The increase in the mesh refinement did not result in clearer boundaries with the bi-linear 4-node quad elements. Also, the bi-linear elements resulted in a checker-board pattern. Although, smooth shapes with sharp boundaries are obtained using B-spline 9 node and 16 node elements, the optimal geometry is different from those obtained using a sparse mesh. It can be observed that the mesh discretization does have an effect on the optimum

topology designs. B-spline elements do not have trouble in representing sharp boundaries even with a sparse mesh as against the traditional bi-linear Q4 elements.

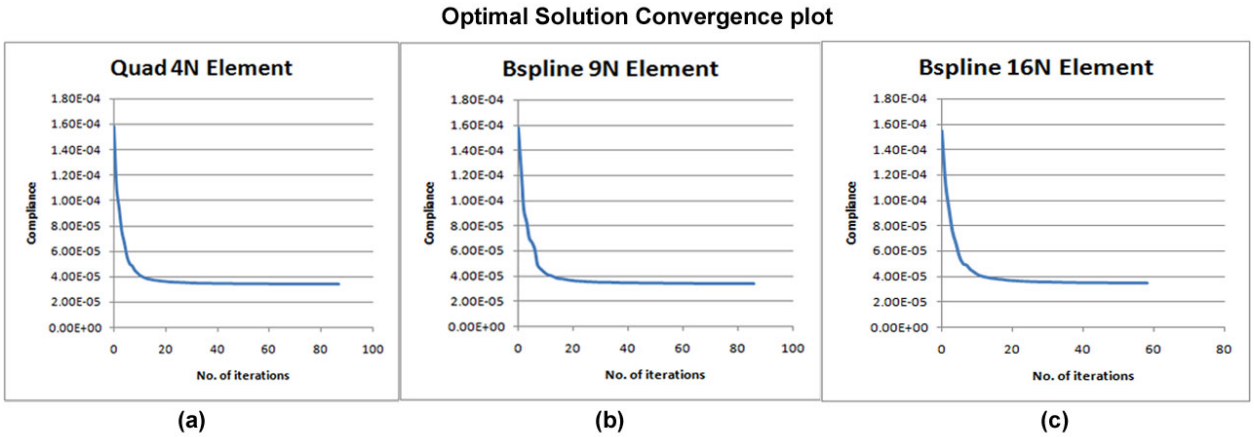

Figure 4-5 Compliance convergence plot for L-shaped structure for a mesh size of 70 x 70 (a) Quad 4N element (b) B-spline 9N element (c) B-spline 16N element

A convergence plot of the optimal solution for bi-linear Q4, B-spline 9-node, B-spline 16-node elements is shown in Figure 4-5. The value of the compliance for each iteration is plotted. The values of the compliance of the final optimal structure along with the number of iterations are tabulated in Table 4-1.

Table 4-1 Compliance convergence results for the L-shaped structure

Element type	Mesh density	Compliance	Iterations to converge
Bilinear Quad 4-node elements	70 x 70	3.397E-5	87
B-spline 9-node elements	70 x 70	3.421E-5	86
B-spline 16-node elements	70 x 70	3.503E-5	58

The compliance convergence plot indicates that the B-spline 9N has a convergence rate of the order of the bilinear quadrilateral elements. But B-spline16N elements have a faster convergence rate towards the optimal solution than B-spline 9N

elements and the bilinear quadrilateral elements. B-spline elements are thus superior in representing smooth boundaries even with a sparse mesh.

Cantilever Plate

To show the influence of using B-spline elements for analyzing structures in which shear deformations cannot be neglected, in this example, we consider a cantilever plate with shear loading. The topology optimization of a cantilever plate for minimum compliance with a constraint on the weight of the structure is performed

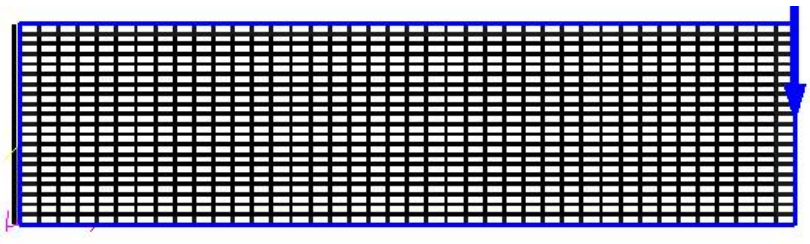

Figure 4-6 Plane stress model of a cantilever plate with a 40 x 20 mesh

A rectangular cantilever plate of dimensions *8.0 x 2.0 m* is subjected to a shear load of 100 N applied at the midpoint of the right edge of the plate. The structure is constrained along the left edge of the plate. The material of the plate is assumed to be steel with the modulus of elasticity equal to 200 GPa and the Poisson's ratio of 0.3. The plane stress model of the cantilever plate along with the loads and boundary conditions is shown in the Figure 4-6. The original domain has been discretized with a sparse mesh of 40 x 20.

Results for the cantilever problem obtained using 99-line Matlab code by *Sigmund* [32] is shown in Figure 4-8. A mesh size of 40 x 20 elements similar to our analysis and a filter radius of 0.1 is used. Bilinear Q4 elements are used for the analysis and it can be observed that the topology obtained is filled with checkerboards.

Figure 4-7 Results from Sigmund's 99 line Matlab code for the cantilever plate problem using a mesh size of 40 x 20 and filter radius of 0.1

The topology results of the optimal designs obtained using the shape density function approach and IBFEM are shown in Figure 4-8. The topology designs are obtained using bilinear 4 node quad, B-spline 9 node and B-spline 16 node elements. SIMP interpolation method with the penalty parameter $p = 3$ for the density function and the allowable material volume fraction of 0.6 is used.

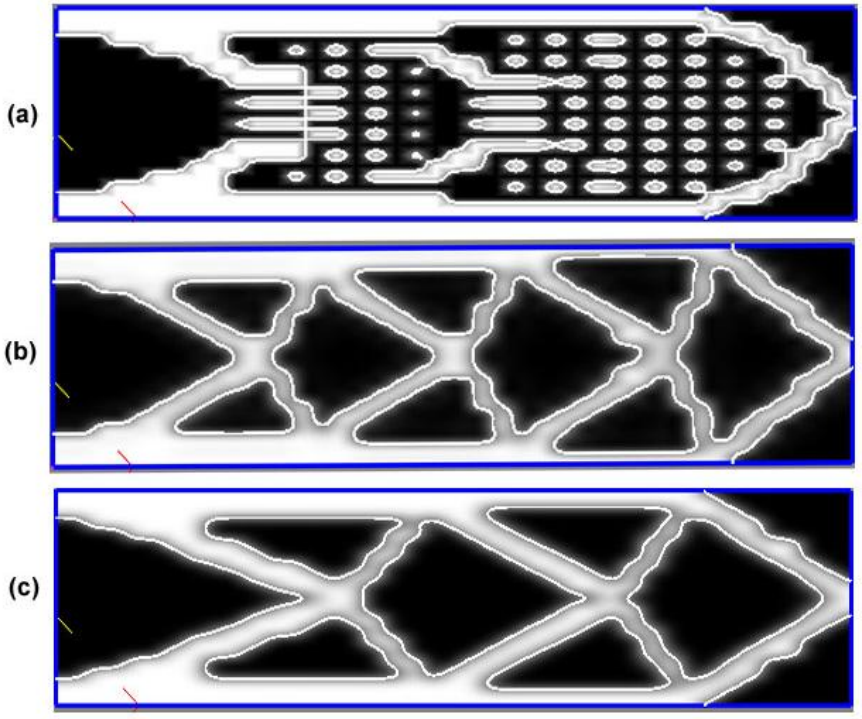

Figure 4-8 Topology optimization results for the cantilever beam with a shear load using a 40 x 20 mesh and volume fraction of 0.6 (a) Quad 4N element (b) B-spline 9N element (c) B-spline 16N element

It can be observed that the 4-node quadrilateral elements have trouble in even converging to a well defined shape and resulted in a checkerboard pattern with a sparse mesh. Since the cantilever plate problem is dominated by shear deformation, the quality of the solution for the structural analysis obtained using Q4 elements is extremely poor. This resulted in a checkerboard pattern without clearly defined boundaries. A similar observation can be made with the results obtained using 99-Matlab code by *Sigmund* [32]. On the other hand, the B-spline 9N and B-spline 16N elements converged to well-defined shapes with smooth boundaries with B-spline 16N elements resulting in boundaries with minimal wriggles. The element size was chosen appropriately according to the volume fraction value used in the problem. The element size has to be comparable to the thickness of the geometry represented to obtain well-defined shapes. B-spline elements demonstrate the ability to represent well-defined, smooth shapes even with a coarse mesh as compared to Q4 elements which failed to result in a well-defined shape.

Bracket Design

Design of a bracket structure is one of the commonly used examples of topology optimization. The topology optimization on a bracket design for compliance minimization with a constraint on the weight of the structure was performed.

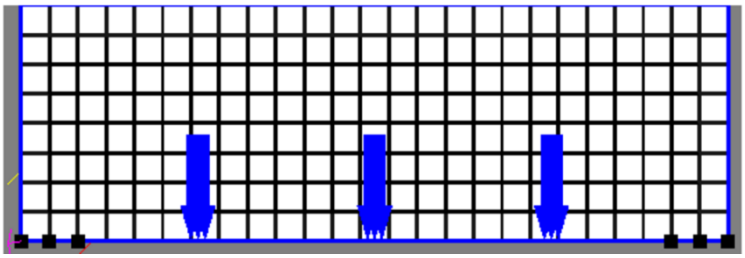

Figure 4-9 Plane stress model of the feasible domain for a bracket design

A rectangular design domain of dimensions *300 x 100 m* is subjected to point forces at various sections of the domain and is constrained on the two ends of the domain. The material is assumed to be steel with the modulus of elasticity equal to 200 GPa and the Poisson's ratio of 0.3. The plane stress model of the feasible design domain along with the loads and boundary conditions is shown in the Figure 4-9. The original domain has been discretized with a sparse mesh of 25 x 8.

The topology results of the optimal designs are shown in Figure 4-10. The topology designs are obtained using bilinear 4 node quad, B-spline 9 node and B-spline 16 node elements. SIMP interpolation method with the penalty parameter $p = 3$ for the density function and the allowable material volume fraction of 0.6 is used.

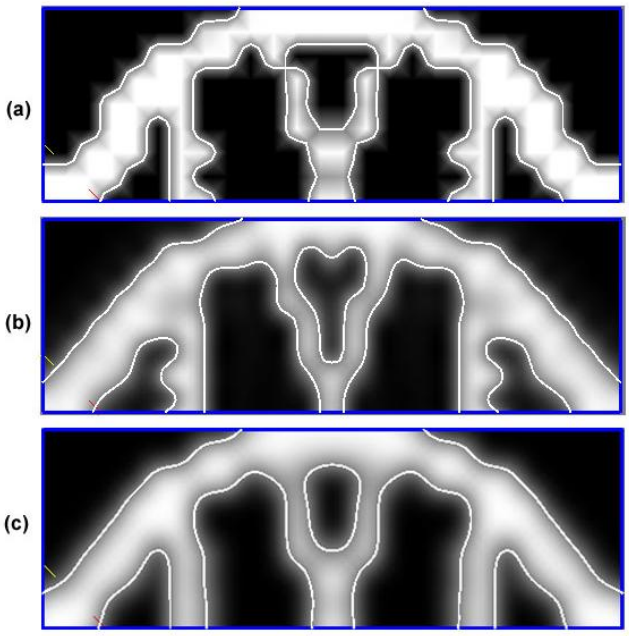

Figure 4-10 Topology Optimization results for the bracket design using a 25 x 8 mesh and volume fraction of 0.4 (a) Quad 4N element (b) B-spline 9N element (c) B-spline 16N element

It can be observed that the Q4 elements result in a shape represented by boundaries that are not smooth when compared to the B-spline 9N and B-spline 16 N

elements. The advantage of using B-spline elements with a sparse mesh is again demonstrated in this example.

Michell Type Structure

Minimum compliance design on Michell-truss type structure is considered in this section. A rectangular feasible domain with a circular hole as the support is considered. A shear force is applied at the middle of the right edge. A volume fraction of 0.8 and a polynomial power of $p = 3$ has been used to obtain the optimum topologies. The material is assumed to be of steel with the modulus of elasticity equal to 200 GPa and Poisson's ratio of 0.3. The feasible domain with loads and boundary conditions is shown in Figure 4-11 (a).

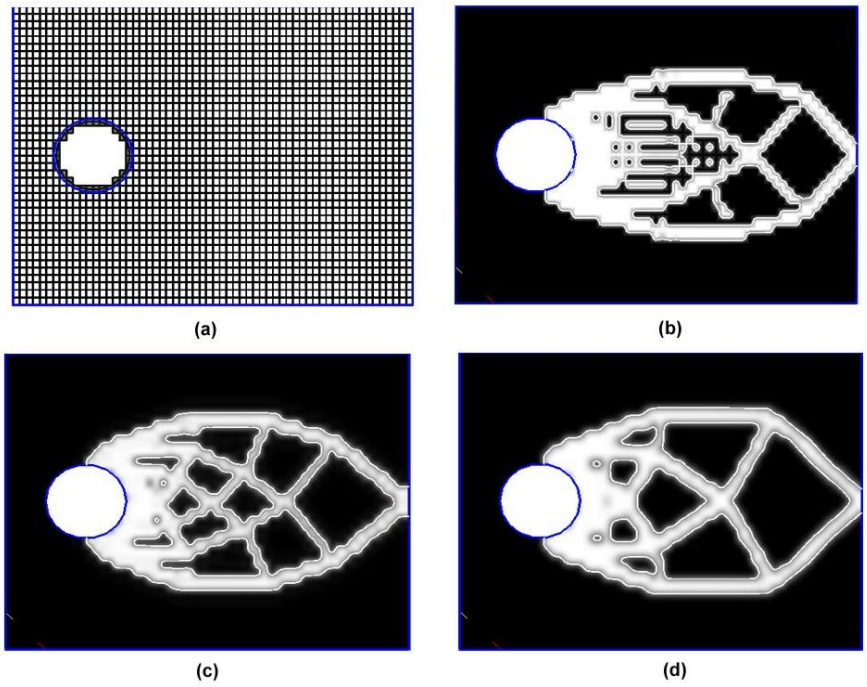

Figure 4-11 Optimal topologies for Michell-truss type structure with a mesh of 60 x 40 elements (a) Feasible domain (b) Quad 4-node element (c) Quadratic B-spline element (d) Cubic B-spline element

The topology results using bilinear 4-node quadrilateral elements, B-spline quadratic 9-node elements and B-spline cubic 16-node elements with a sparse mesh density of 60 x 40 are shown in Figure 4-11. Michell-truss type structures often result in topologies with fine microstructure representation with highly refined mesh. Q4 elements have trouble in representing the microstructure for the given sparse mesh density. On the other hand, the final topologies obtained using B-spline elements have smooth boundaries and are free from checkerboard patterns.

Rocker Arm Design

An example of a rocker arm design for the seat of a car is considered here. The feasible design domain is shown in Figure 4-12 (a). The rocker arm pivots about the hole *C* and is supported by pins at *B* and *D*. A force of magnitude 1000 is applied at the centre of the hole A in the negative x-direction. A sparse mesh of 10 x 20 elements is chosen. The material of the rocker arm is assumed to be steel with modulus of elasticity 200 GPa and Poisson's ratio of 0.3. A polynomial power of $p = 3$ and a volume fraction of 0.7 are used.

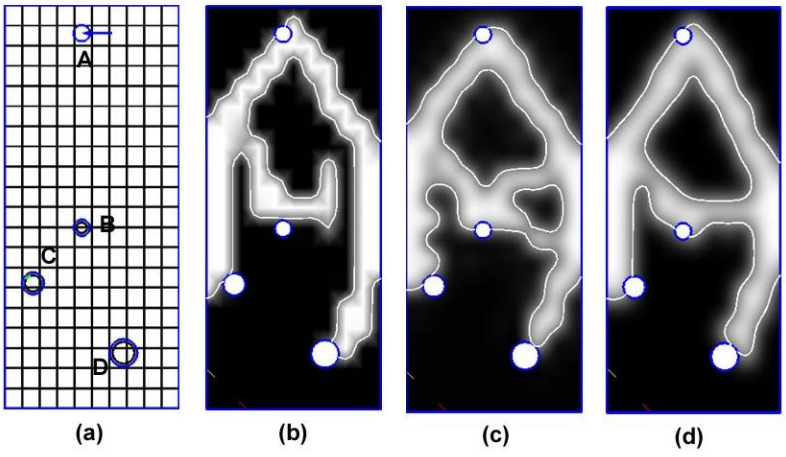

Figure 4-12 Optimal topologies for the design of a rocker arm for a mesh size of 10 x 20 and a volume fraction of 0.7 (a) Feasible domain (b) Quad 4N elements (c) B-spline 9N elements (d) B-spline 16N elements

The final topologies obtained using bilinear quadrilateral element and the B-spline elements are shown in the Figure 4-12 (b – d). Quad 4N elements have trouble in representing a connected shape with such a sparse mesh. On the other hand, well connected shapes with smooth boundaries are obtained using B-spline elements.

CHAPTER 5
COMPLIANT MECHANISM DESIGN

Introduction

Compliant mechanisms are mechanical devices in which elastic deformations produce motion as opposed to rigid body mechanisms which attain their motion from hinges, bearings and sliders. In the design of conventional rigid body mechanisms, elastic deformations are considered undesirable. On the other hand, compliant mechanisms are intentionally designed to be flexible to perform useful work. The advantages of compliant mechanisms are that they are single-piece, joint-less mechanisms which can be constructed by simple manufacturing process unlike the rigid body mechanisms. The reduction in the number of parts when compared to the rigid body mechanisms reduces the weight, manufacturing cost and eliminates the need for assembly. Fewer rigid body parts help reduce friction, wear, backlash and noise. The flexibility of the parts of a compliant mechanism allows it to absorb overloads without structural failure.

One of the important objectives in the design of compliant mechanisms is the relationship between the input and output displacements or forces which can be specified by means of geometric advantage or mechanical advantage. The compliant mechanism designs should satisfy both the kinematic and structural requirement. As an example, Figure 5-1 (a) shows a compliant mechanism design to grip a work piece. The compliant mechanism should be flexible enough to deform under the force F_A. On the other hand, once the mechanism comes in contact with the work piece, it should resist further deformation as shown in Figure 5-1 (b).

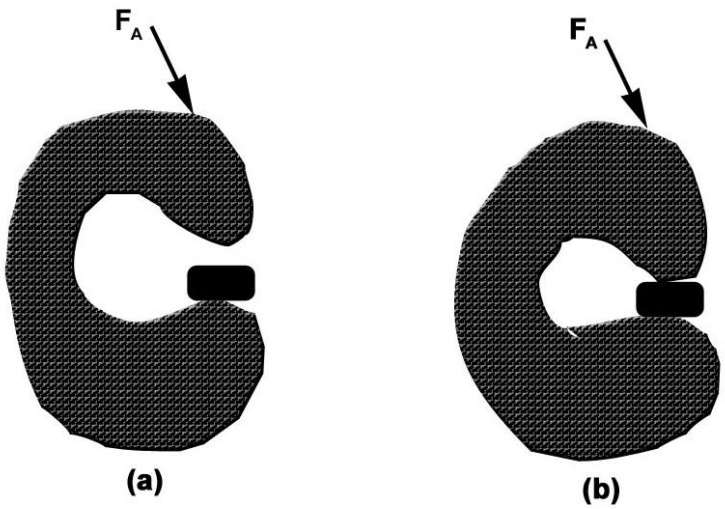

Figure 5-1 Compliant mechanism design example

There are two approaches to compliant mechanism design, the kinematic synthesis approach and the continuum synthesis approach. *Midha et al.* [36] developed the kinematic synthesis approach for the design of compliant mechanisms. Based on the rigid-body kinematics, a basic configuration of the design is obtained. It is then converted into a partially compliant mechanism with flexible segments or fully compliant mechanism with lumped compliance. Rigid-body mechanism analysis is used to discuss the kinematic properties such as degree of compliance of compliant mechanisms by *Her and Midha* [37]. Given a rigid-body kinematic chain, they present a methodology to derive all possible compliant mechanism designs from the chain. *Murphy et al.* [38] used graph theory to design compliant mechanisms and determined the number of flexural segments, topological connectivity and kinematic inversions. *Howell and Midha* [39] developed a pseudo-rigid model to design compliant mechanisms with small flexible sections when compared to the relatively rigid segments. The method uses a large-deflection finite element type algorithm. Using the pseudo-rigid model, *Howell and*

Midha [40] developed a loop-closure method to design compliant mechanisms. The pseudo-rigid model simplifies the analysis of compliant mechanisms by determining an equivalent rigid-body mechanism that accurately models the kinematic characteristics of a compliant mechanism. *Howell et al.* [41] simplified the modeling of force/deflection relationships of large-deflection members of a compliant mechanism.

The first application of topology optimization methods to compliant mechanism design were carried out by *Ananthasuresh et al.* [42]. They developed a continuum based approach using the homogenization method to design compliant mechanisms. Systematic methods have since been developed to design and synthesize compliant mechanisms. *Ananthasuresh and Kota* [43] and *Ananthasuresh et al.* [44] discuss a systematic synthesis method of compliant mechanisms and its application to micro-electro-mechanical systems (MEMS).

Sigmund [45] and *Larsen et al.* [46] developed a modified approach using microstructure design of materials to synthesize the compliant mechanism design. Sigmund [47] initiated an approach in which the output loads were modeled by a spring. This allowed full control over the input-output behavior. *Lau et al.* [48] used functional specifications such as maximizing geometric advantage or mechanical advantage as objectives to design compliant mechanisms.

In most of the structural optimization problems, a linear elastic response is assumed. While this assumption is valid for a wide variety of problems, it is not valid for structures undergoing large displacements. *Bruns and Tortorelli* [49] used the elastic structural analysis which could accommodate geometric and material non-linearities in the design of compliant mechanisms. *Pedersen et al.* [50] used topology optimization as

a synthesis tool to design large-displacement compliant mechanisms and path generating mechanisms.

Frecker et al. [51] developed another approach to solve multi-criteria optimization problem to design compliant mechanism. Since the design involves conflicting objectives which should satisfy both the kinematic and structural requirements, maximization of ratios of two energies based on two different finite element problems was used. However, the mechanism designs obtained were stiffer and hence lacked sufficient flexibility. *Nishiwaki et al.* [52] describes topology optimization method to design compliant mechanisms using the homogenization method. This method also uses a multi-objective objective criterion for the design of compliant mechanisms based on ratios of energies. *Frecker et al.* [53] developed topology optimization formulations to handle multiple output requirements in the design of compliant mechanism designs. *Kota et al.* [54] developed a methodology to design joint-less mechanisms with distributed compliance and tested the methodology for a MEMS application.

Compliant mechanism designs have diversified applications. One of the important applications of compliant mechanisms is in the design of MEMS. MEMS cannot be manufactured using typical assembly processes and may not make use of bearings and hinges since even small frictional forces will dominate at such a small scale. The compliant mechanisms also have application in the design of adaptive structures in which the underlying structure is made up of numerous actuators to reconfigure itself to effect a change in the shape of an attached entity. The underlying structure, if designed as a compliant mechanism, which will inherently be adaptive, the final design would be simple and more energy efficient.

Design Objectives Studied

In this thesis, a number of design objective functions to synthesize compliant mechanisms were studied. A summary of a few of them are listed below.

1. *Frecker et al.* [51] considered a multi-objective formulation to synthesize compliant mechanisms by introducing the concept of mutual potential energy. Both the deflection and the mean compliance of the mechanism are considered to take into account both the kinematic requirements and the structural requirements simultaneously. Two loading conditions treated as two different finite element models are considered. The first loading condition can be considered to satisfy kinematic requirements. Maximum flexibility can be posed as a maximization of deflection at certain points in a specific direction. Maximization of deflection at the output points due to forces f_a applied at input points and virtual forces f_b applied at the output points in the direction of deflection is equivalent to maximizing the mutual potential energy. The second loading condition is considered for structural requirements. Minimization of compliance of the structure is computed by fixing the points the input points in the first loading condition and applying forces f_b in the opposite direction at the output points where maximum deflection is desired. The Objective function can be then defined as:

$$\min f = \frac{\text{compliance only when } f_b \text{ acts}}{\text{Mutual potential energy when both } f_a \text{ and } f_b \text{ acts}} \tag{5-1}$$

$$\min f = \frac{f_b u_b}{f_b u_a} \tag{5-2}$$

2. *Kota et al.* [54] posed a two-part problem formulation to satisfy both the kinematic and structural requirements. The first part of the problem formulation is called the

"mechanical design" in which the kinematic requirements are met by maximizing geometric advantage of the mechanism to generate desired motion. The second part of the problem formulation is called the "Structural design" in which the structural requirements are met by minimizing the compliance or minimizing the strain energy of the system. The objective function is given by:

$$\max f = \frac{\text{Geometric Advantage}}{\text{Strain Energy}} \tag{5-3}$$

3. *Chen et al*. [55] posed a new objective for the design of compliant mechanisms by specifying a desired geometric advantage for the mechanism. The objective function is given as:

$$\text{Minimize, } J_p = \left(\frac{\Delta_{out}}{\Delta_{in}} - A\right)^2 \tag{5-4}$$

Here A is the desirable value of the geometric advantage and Δ_{out} and Δ_{in} are the output and input displacements.

4. *Lau et al.* [48] posed an alternative formulation based on functional specifications to design compliant mechanisms instead of using the concepts of minimum compliance or maximum mutual compliance. The objective function can be formulated as given below,

$$\text{Maximize, } MA = \frac{F_{out}}{F_{in}} \tag{5-5}$$

$$\text{Maximize, } GA = \frac{\Delta_{out}}{\Delta_{in}} \tag{5-6}$$

$$\text{Max work ratio} = \frac{F_{out} \cdot \Delta_{out}}{F_{in} \cdot \Delta_{in}} = \text{MA} \times \text{GA} \tag{5-7}$$

Objective Function

An objective function to synthesize the desired path of the compliant mechanism has been used in this thesis. The goal is to make the output port move through a set of *N* precision points for *N* given input displacements. An objective function can thus be formulated as an error function:

$$\text{Minimize}, \prod(\phi) = \sum_{n=1}^{\text{N data points}} \left[u_{out,n} - u^{*}_{out,n} \right]^2 \tag{5-8}$$

$$\text{subject to: } M(\phi) = \int_{\Omega} \phi \, d\Omega \leq M_0 \tag{5-9}$$

$$\int_{\Omega_0} \{\delta\varepsilon\}^T \left[D(\phi) \right] \{\varepsilon\} \, d\Omega = \int_{\Gamma} \{\delta u\}^T \{ f \} \, d\Gamma \tag{5-10}$$

$$\phi_{th} \leq \phi \leq 1 \tag{5-11}$$

Here $u_{out,n}$ and $u^{*}_{out,n}$ are the actual and prescribed output displacements corresponding to the input displacements $u_{in,n}$. When the error function is equal to zero, the output port undergoes the desired path.

Sensitivity Analysis

The density-material property relation should be defined such that if the density is decreased in a region, the stiffness should decrease correspondingly causing the material to become weaker in that region. This could be achieved if the gradient of the objective function with respect to the design variables, $\frac{\partial L(\phi)}{\partial \phi_i}$ is negative. The optimization algorithm would therefore decrease the densities in those regions where the material is underutilized resulting in new holes to be created or shrinking of existing boundaries inwards. The gradient of the objective function is given by,

$$\frac{\partial L(\phi)}{\partial \phi_i} = \sum_{m=1}^{\text{No.of data pts}} 2 * \left[\sum_{j=1}^{npe} N_j u_j - u_m^* \right] \left[\sum_{k=1}^{npe} N_k \frac{\partial u_k}{\partial \phi_i} \right] \tag{5-12}$$

The gradient of the nodal displacements can be computed by the standard design sensitivity analysis methods. The equilibrium equations are reduced to a set of linear simultaneous equations in a finite element model which is given by,

$$[K]\{U\} = \{F\} \tag{5-13}$$

$[K]$ is the stiffness tensor, $\{U\}$ contains the nodal displacements u_i and $\{F\}$ is the load vector. The gradient of u_i can be computed by differentiating the equation (5-13) with respect to the density ϕ,

$$[K]\frac{\partial \{U\}}{\partial \phi_i} + \frac{\partial [K]}{\partial \phi_i}\{U\} = 0 \tag{5-14}$$

or $$\frac{\partial \{U\}}{\partial \phi_i} = -[K]^{-1}\frac{\partial [K]}{\partial \phi_i}\{U\} \tag{5-15}$$

Substituting for $\frac{\partial \{U\}}{\partial \phi}$ in (5-12), we get,

$$\frac{\partial L(\phi)}{\partial \phi_i} = \sum_{m=1}^{\text{No.of data pts}} 2 * \left[u_m^* - \sum_{j=1}^{npe} N_j u_j \right] \left[\sum_{k=1}^{npe} N_k [K]^{-1} \frac{\partial [K]}{\partial \phi_i}\{U\} \right] \tag{5-16}$$

Now, constructing the adjoint variable λ for all the nodes in the elements for which output displacements are specified, we have,

$$\lambda_i = 2 * \left[u_d^* - \sum_{j=1}^{npe} N_j u_j \right] N_i [K]^{-1} \tag{5-17}$$

Let $$\text{xbar} = 2 * \left[u_d^* - \sum_{j=1}^{npe} N_j u_j \right] N_i \tag{5-18}$$

Therefore we can solve for λ as given below,

$$[K]\{\lambda\} = \{\text{xbar}\} \tag{5-19}$$

Once λ is obtained, the gradient of the objective function can be computed as given below,

$$\frac{\partial L(\phi)}{\partial \phi_i} = \lambda \frac{\partial [K]}{\partial \phi_i}\{U\} \tag{5-20}$$

Results

Gripper Mechanism Design

As an example, let us consider the design of a mechanical gripper. The mechanism is supported at the two corners on its left edge and input forces of magnitude 50000 N are applied in the middle of the left edge as shown in Figure 5-2. Vertical displacements are expected at the points A and B in right open jaw of the mechanism to grip the work-piece. Forces of magnitude 5000 N are applied at the points A and B, where displacements are expected, to model the resistance of the work-piece once the mechanism comes in contact with the work-piece.

The size of the design domain is 5 x 5 m as shown in Figure 5-2. Displacements of magnitude 0.00025 are prescribed at two corner points A and B and displacements of magnitude 0.000025 are prescribed at the points where the input forces are applied. The material of the domain is assumed to be steel with modulus of elasticity equal to 200 GPa and the Poisson's ratio of 0.3. The original domain has been discretized with a sparse mesh of 30 x 30 elements.

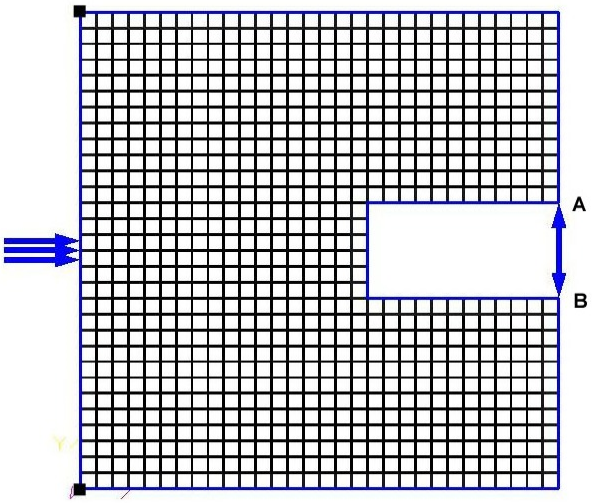

Figure 5-2 Feasible domain for gripper mechanism design with a 30 x 30 mesh

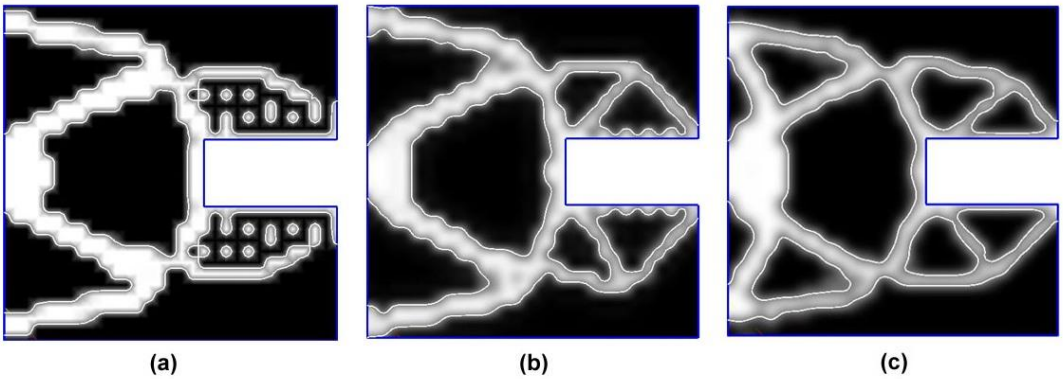

Figure 5-3 Topology results for a mechanical gripper design with a 30 x 30 mesh using (a) Quad 4N elements (b) B-spline 9N elements (c) B-spline 16N elements

The topology results of the optimal designs are shown in Figure 5-3. The topology designs are obtained using bilinear 4 node quad, B-spline 9 node and B-spline 16 node elements. SIMP interpolation method with the penalty parameter $p = 4$ for the density function and the allowable material volume fraction of 0.7 is used. It can be observed that with the use of sparse mesh, the bilinear Quad 4-noded elements results in a shape that is not well connected and have problems in smooth representation of the

boundaries. The optimal geometries obtained using B-spline elements are well connected and smoother without any checkerboard patterns.

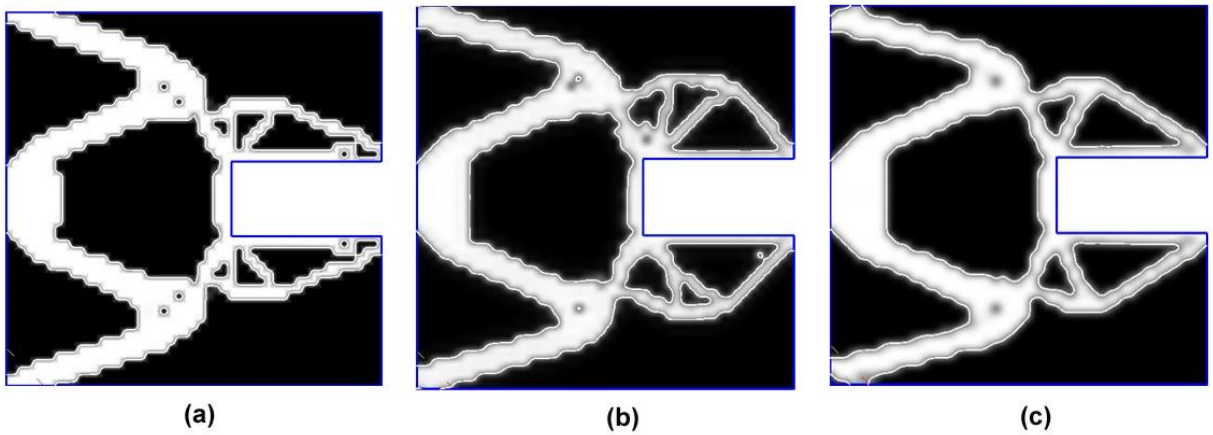

Figure 5-4 Topology results for a mechanical gripper design with a 50 x 50 mesh using (a) Quad 4N elements (b) B-spline 9N elements (c) B-spline 16N elements

The topology results with an increased mesh refinement of 50 x 50 elements are shown in Figure 5-4 for Q4, B-spline 9N and B-spline 16 N elements. It can be observed that with the increase in mesh refinement, even the Q4 elements converge to a better smooth shape and the B-spline elements also converge to better smooth shapes.

To evaluate the validity of the designs obtained using B-spline elements in IBFEM, finite element models similar to the optimal designs were created using the commercial FEA package ABAQUS. The finite element model of the optimal design along with the loads and boundary conditions are shown in Figure 5-5 (a). 4-node linear shell elements are used for the analysis. A superimposed image of the deformed and un-deformed shapes of the geometry is shown in Figure 5-5 (b). The deformation of the mechanism was indeed in the direction as intended. Thus, the designs obtained for the gripper mechanism are indeed valid.

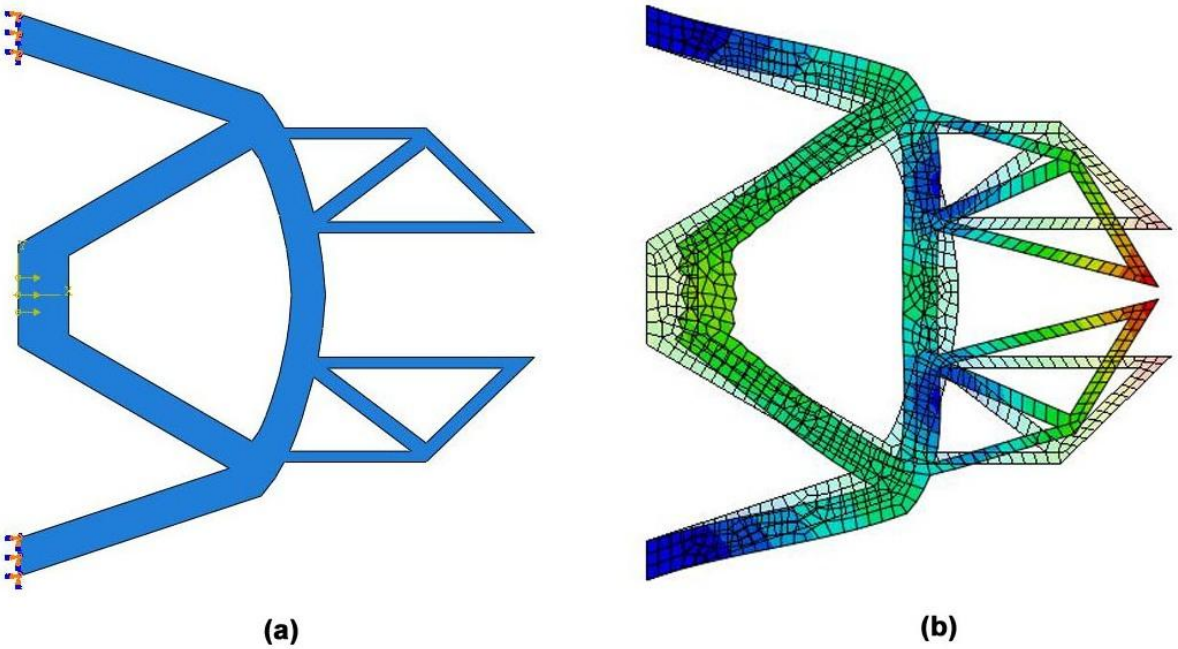

Figure 5-5 Results from ABAQUS for the gripper mechanism (a) FE Model of the gripper mechanism with loads and boundary conditions (b) Deformed shape of the gripper mechanism

Displacement Inverter Mechanism Design

The feasible domain for the design of a displacement inverter mechanism is shown in Figure 5-6. The mechanism is supported at the two corners along its left edge and input forces of magnitude 50000 N are applied at the middle of the left edge as shown in Figure 5-6. Displacements are expected at the output ports at the middle of the right edge in the negative x-direction. Forces of magnitude 5000 N are applied at the output ports in the direction opposite to the direction in which displacements are required.

The size of the design domain is 5 x 5 m as shown in Figure 5-6. Displacements of magnitude -0.000001 (in the negative x-direction) are specified at output ports and displacements of magnitude 0.00001 are specified at the points where the input forces are applied. The material of the domain is assumed to be steel with modulus of elasticity

equal to 200 GPa and the Poisson's ratio of 0.3. The original domain has been discretized with a sparse mesh of 30 x 30 elements.

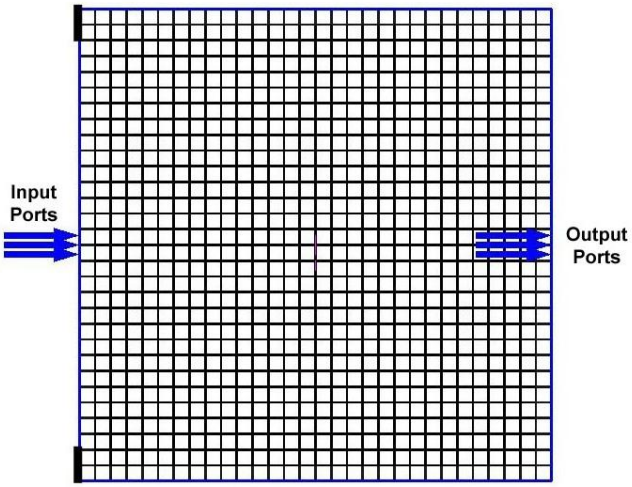

Figure 5-6 Feasible domain for displacement inverter design with a 30 x 30 mesh

The topology results of the optimal designs for the inverter mechanism are shown in Figure 5-7. The topology designs are obtained using bi-linear 4 node quad, B-spline 9 node and B-spline 16 node elements. SIMP interpolation method with the penalty parameter $p = 4$ for the density function and the allowable material volume fraction of 0.8 is used.

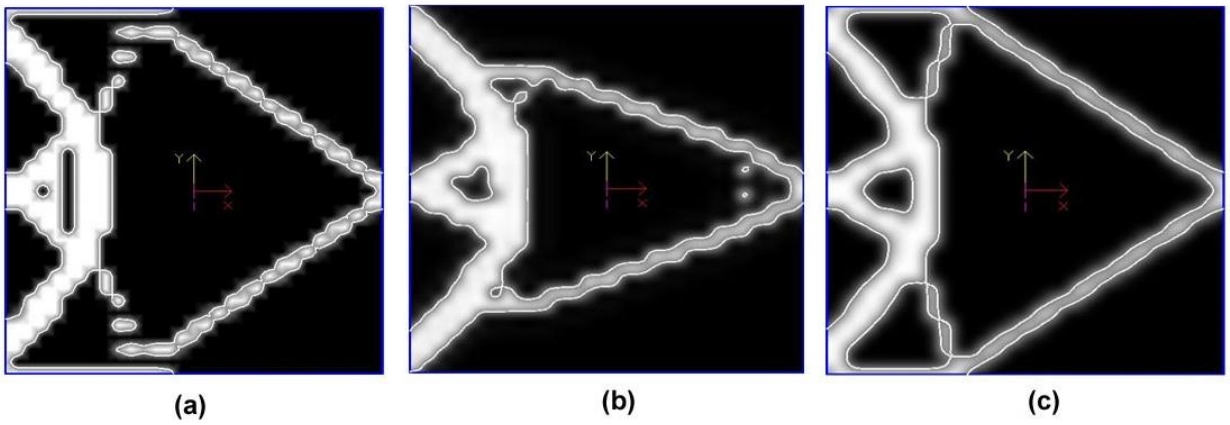

Figure 5-7 Topology results for a displacement inverter design with a 30 x 30 mesh using (a) Quad 4N elements (b) B-spline 9N elements (c) B-spline 16N elements

With the use of a sparse mesh of 30 x 30 elements, the design obtained using bilinear quad 4-noded elements is not well connected and the boundary representation is not smooth. On the other hand, B-spline elements result in geometries that have smooth and clear boundaries. Checkerboard pattern is inherently eliminated in B-spline elements.

The second part of this example is performed on a similar feasible domain with a refined mesh discretization. A refined mesh discretization of 50 x 50 elements was used to validate if the topologies obtained would be any different from the topologies obtained using a sparse mesh. The topology results of the optimal designs are shown in Figure 5-8. With a refined mesh, the design obtained using bilinear Quad 4-node elements has considerably improved with clear boundaries. B-spline elements also result in geometries that have smooth and clear boundaries.

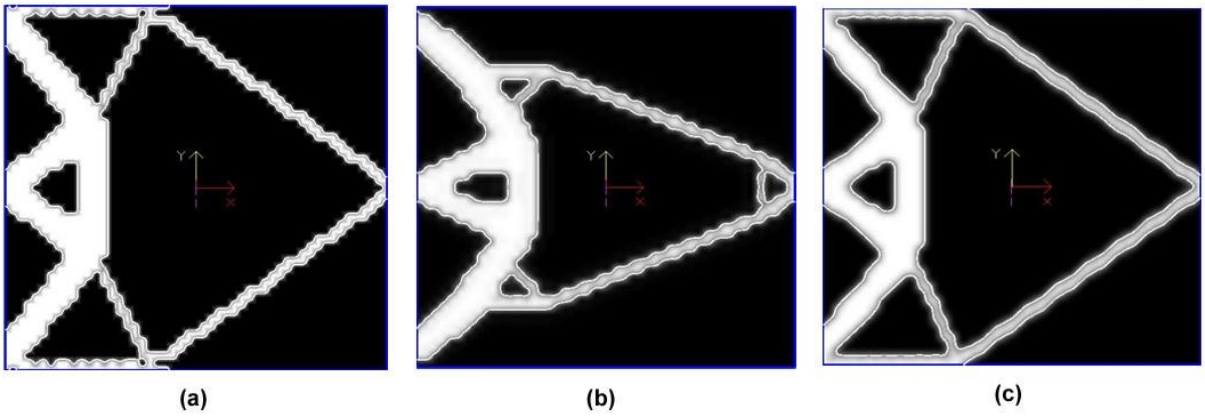

Figure 5-8 Topology results for a displacement inverter design with a 50 x 50 mesh using (a) Quad 4N elements (b) B-spline 9N elements (c) B-spline 16N elements

The designs obtained using B-spline elements in IBFEM were validated using a commercial FEA package to evaluate the working of the displacement inverter mechanism. Commercial FEA package ABAQUS is used to evaluate the designs. The

finite element model of the optimal design of the displacement inverter mechanism along with the loads and boundary conditions is shown in Figure 5-9 (a). 4-node linear shell elements are used for the analysis. Figure 5-9 (b) shows the superimposed image of the deformed and un-deformed geometries. The tip of the inverter is expected to move in the negative x-direction when a force is applied in the positive x-direction on left edge. The deformed shape shows that the designs obtained for the inverter mechanism are valid.

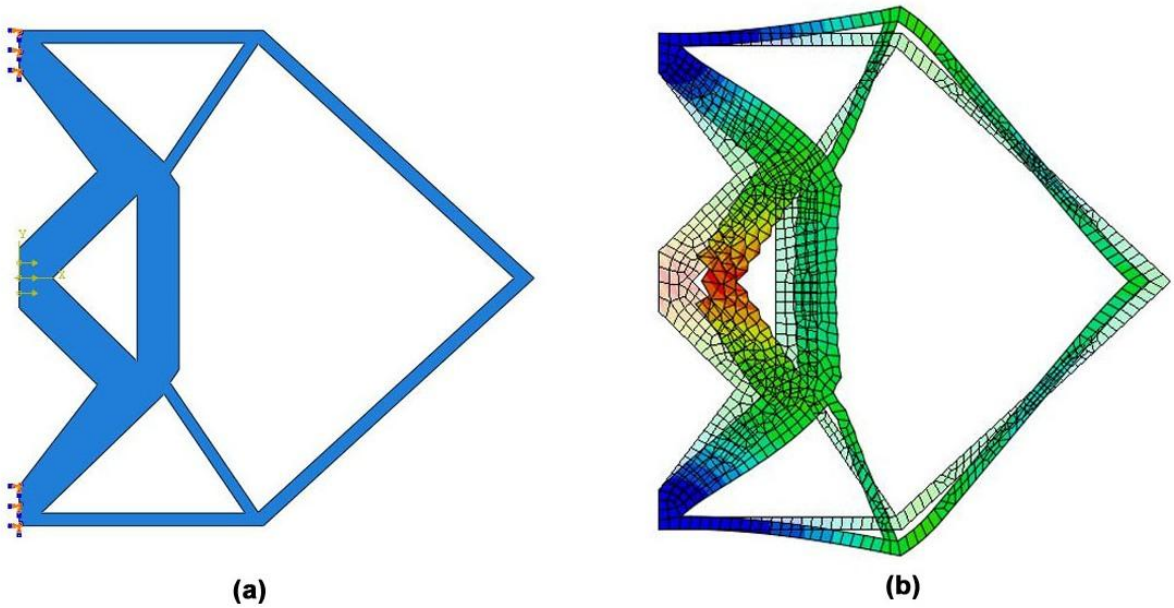

Figure 5-9 Results from ABAQUS for the inverter mechanism (a) FE Model of the inverter mechanism with loads and boundary conditions (b) Deformed shape of the inverter mechanism

Flapping Wing Mechanism

A flapping wing mechanism for a micro air vehicle is to be designed to obtain large displacements at the tip of the wings. The wings will be activated by an electro-magnetic actuator placed in the fuselage. The shape of the holder for the electrostatic actuator is to be obtained using topology optimization for design of compliant mechanisms. The feasible domain for the flapping mechanism with a mesh size of 70 x 35 elements is

shown in Figure 5-10. A polynomial power of $p = 3$ and a volume fraction of 0.5 is used to obtain the optimum topology results. The material of the structure is assumed to be steel with a modulus of elasticity 200 GPa and Poisson's ratio of 0.3. Displacements of magnitude 2.0 E-5 are specified at the wing tips and the entire structure is fixed at the centre of the bottom edge.

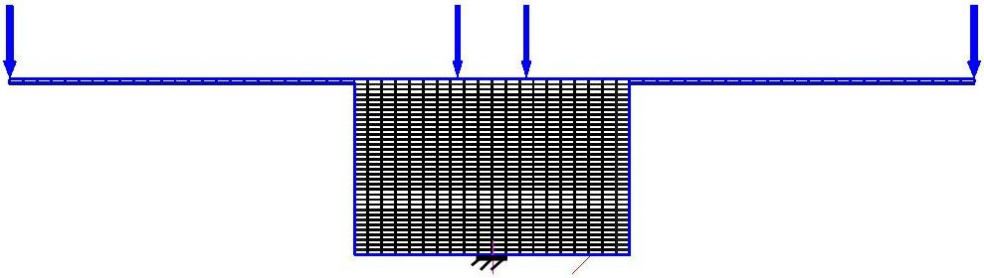

Figure 5-10 Feasible domain for a flapping wing mechanism with 70 x 35 elements

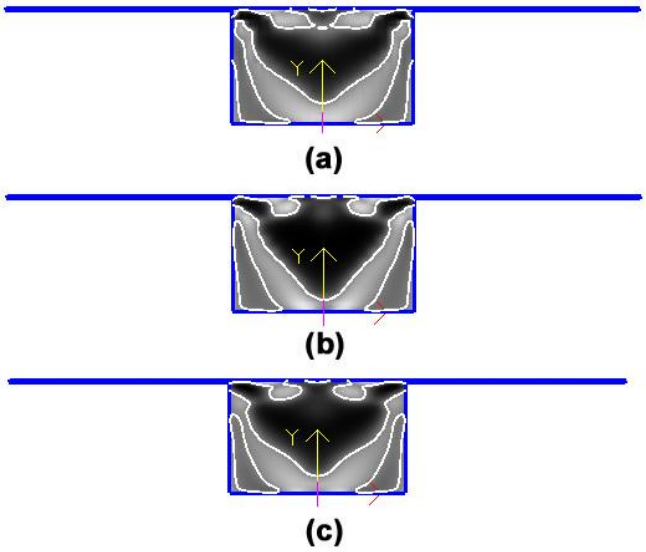

Figure 5-11 Topology results for the flapping mechanism for a 70 x 35 size mesh and a volume fraction of 0.5 (a) Quad 4N elements (b) B-spline 9N elements (c) B-spline 16 N elements

The topology results obtained using bilinear 4-node quadrilateral elements, B-spline 9N elements and B-spline 16N elements are shown in Figure 5-11.

To validate the design of the mechanism obtained using topology optimization, a finite element analysis is performed on the final topology of the structure. Figure 5-12 shows a superimposed image of the deformed shape on the optimum structure. As expected a displacement of 2.0 E-5 is obtained at the wing tips as shown proving the validity of the design.

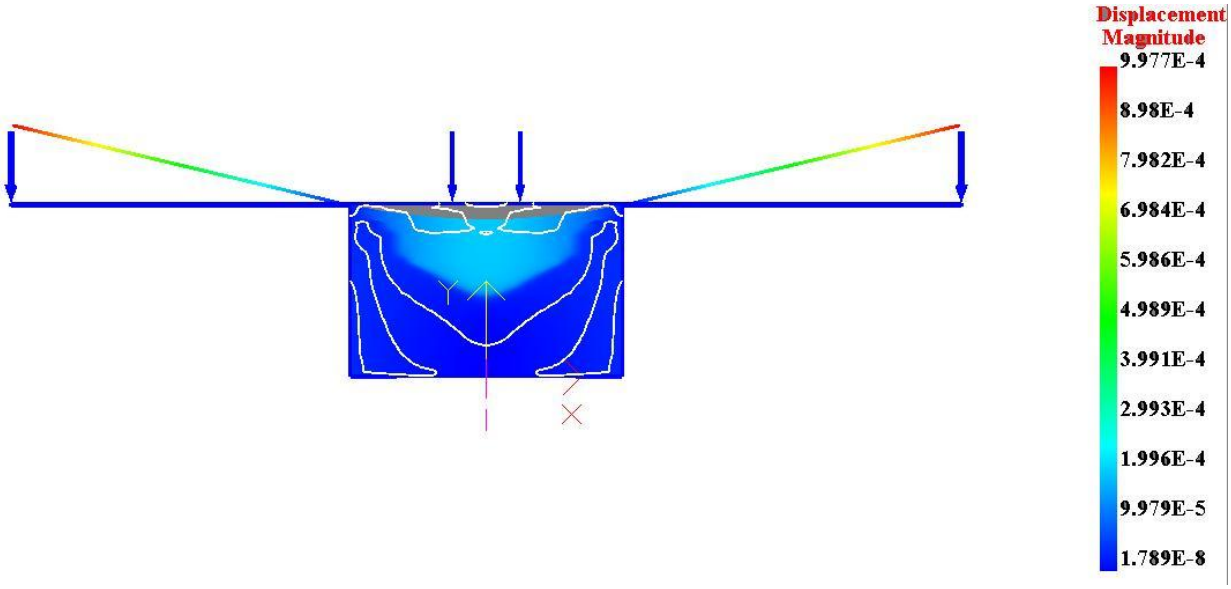

Figure 5-12 Results from a finite element analysis on the optimum structure for the flapping mechanism

B-spline elements thus demonstrate the ability to obtain the optimal shapes even with sparse mesh discretizations when compared with the bilinear quadrilateral elements which required dense mesh discretization to obtain similar optimal shapes.

CHAPTER 6
SMOOTHING SCHEME FOR MESH INDEPENDENT SOLUTIONS

One of the numerical instabilities in the computational results obtained with the material distribution or layout optimization problems is the mesh dependence of the optimal solutions obtained. It is a known fact that the discrete 0-1 topology optimization problem lacks unique solution. It has been observed that there is a general increase in the efficiency of the structure with the introduction of more holes without any changes in the structural volume. Hence, feasible set of solution that can be obtained for a given problem is not limited. Mesh dependence can be defined as a type of numerical instability in which qualitatively different solutions are obtained with different sizes of mesh discretization. With the increase in the mesh density, structural variations in the form of microstructure appear in the optimal topology. The dependence on mesh refinement is shown in Figure 6-1 for a Michell-truss type structure. An increase in the mesh refinement resulted in a much more detailed final optimal structure.

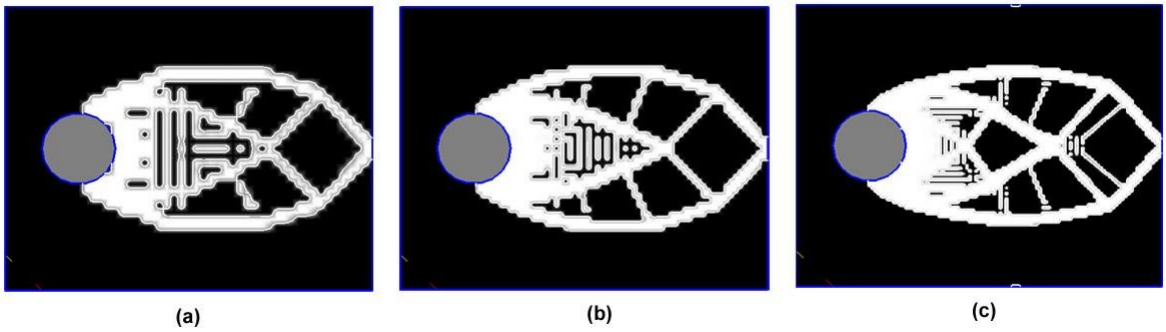

Figure 6-1 Dependence of optimal topology on mesh refinement for a Michell-truss structure using Q4 elements. Solution for a mesh density of (a) 2000 elements (b) 4800 elements (c) 12000 elements

It has been observed that neither the homogenization method nor the SIMP approach can eliminate the mesh dependence on the solutions unless additional techniques are applied. An overview of the various techniques employed in obtaining

mesh independent solutions can be found in *Sigmund and Peterson* [56]. *Zhou et al* [57] developed a methodology to obtain a minimum member size control in the optimum topology and hence obtain solutions that are mesh independent. *Bendsøe and Sigmund* [2] discuss various techniques to enforce mesh independent optimum solutions. They fall into two general categories namely applying constraints to the original optimization problem and applying filters in the optimization algorithm.

In this thesis, a new smoothing scheme to obtain mesh independent optimum topologies is introduced. The method involves minimizing the square of the gradient of the density over the volume of the entire design domain. This is achieved by augmenting the smoothing term as a weighted sum with the original objective function. Minimization of square of the gradient of the density tends to drive the densities of the discrete domain towards a 0-1 design. It tends to minimize the variations in the density over the entire domain. The variations in the density are significant near the boundaries of the structure. The transition of density near the boundaries from the threshold value to almost zero density is quite significant. Therefore, minimization of the square of gradient of density clearly limits the number of holes that can appear in the final topology and results in solutions that are independent of the mesh discretization.

The perimeter of the geometry is the sum of the lengths of all inner and outer boundaries. The number of holes that can appear in the domain can be limited by constraining the perimeter of the domain. Since the transition of density near the boundaries have to be minimized to obtain mesh independent solutions, the method aims at having minimum number of holes and steps along the boundaries. As a result, it indirectly results in constraining the perimeter of the final optimum shape and hence

results in smooth boundaries in the final topology. In addition to obtaining mesh independent solutions with smooth boundaries, it has been observed that the smoothing scheme also results in obtaining solutions that are independent of the type of the elements used for the structural analysis in the optimization process.

Details of the Smoothing Scheme

Objective Function

The smoothing term is augmented to the objective function as a weighted sum in the optimization problem. An appropriate weight *w* has to be chosen depending upon the compliance value of the initial structure. The original optimization problem can be restated as follows,

Minimize, $\prod = F(\phi) + w\int_V \left(\nabla\phi\right)^2 dV$ (6-1)

The gradient of the density over the design domain can be computed as an integral over the volume of the design domain as given below,

$$P = \int_V \left(\nabla\phi\right)^2 dV = \sum_{e=1}^{n_e} \int_{V_e} \left(\sum_{j=1}^{npe} \phi_j \frac{\partial N_j}{\partial x_i} \right)^2 dV \quad (6\text{-}2)$$

Here, ϕ_j is the nodal value of the density and $\frac{\partial N_j}{\partial x_i}$ is the derivative of the nodal shape functions along the x_i direction.

Sensitivity Analysis

The sensitivity of the smoothing term with respect to the nodal density can be computed as given below,

$$\frac{\partial P}{\partial \phi_j} = \int_V 2\left(\nabla\phi\right).\frac{\partial\left(\nabla\phi\right)}{\partial\phi_j}\, dV \quad (6\text{-}3)$$

$$\frac{\partial P}{\partial \phi_j} = \sum_{e=1}^{n_e} \int_{v_e} \left(2(\nabla \phi)_i \cdot \frac{\partial N_j}{\partial x_i} \right) dv \tag{6-4}$$

Results

Element-Type Independent Results

The L-shaped region used for the minimum compliance design in chapter 4 is again considered to demonstrate the capability of the smoothing scheme to yield solutions that are independent of the type of the element used. The plane stress model of the L-shaped region with the dimensions and the mesh discretization is shown in Figure 6-2. A shear load of 200 N is applied along the right edge and the domain is constrained along the top edge. The material of the domain is assumed to be steel with modulus of elasticity equal to 200 GPa and the Poisson's ratio of 0.3. The original domain has been discretized with a sparse mesh of 20 x 20 elements.

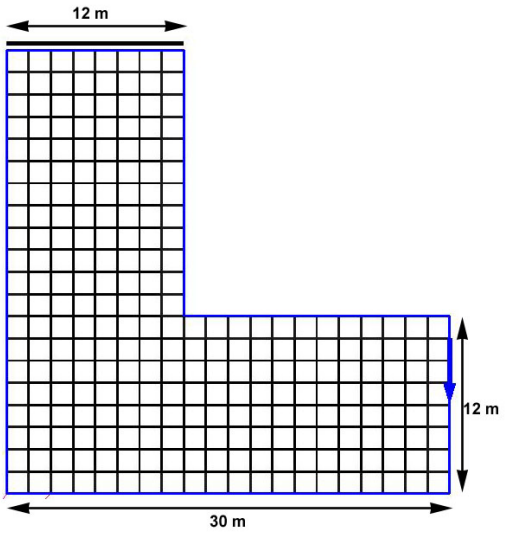

Figure 6-2 Plane stress model of a loaded L-shaped structure with a 20 x 20 mesh

The topology results of the optimal minimum compliance designs along with the smoothing term are shown in Figure 6-3. The topology designs are obtained using B-

spline 9 node and B-spline 16 node elements and the results compared with the results obtained using bilinear 4 node quadrilateral elements. SIMP interpolation method with the penalty parameter $p = 4$ for the density function and the allowable material volume fraction of 0.5 is used.

It was observed in chapter 4 that, for a given mesh size, the topology results obtained using different elements resulted in solutions that were significantly different. Evidently, the inclusion of the smoothing term in the objective function yields solutions having similar topology irrespective of the type of the element used.

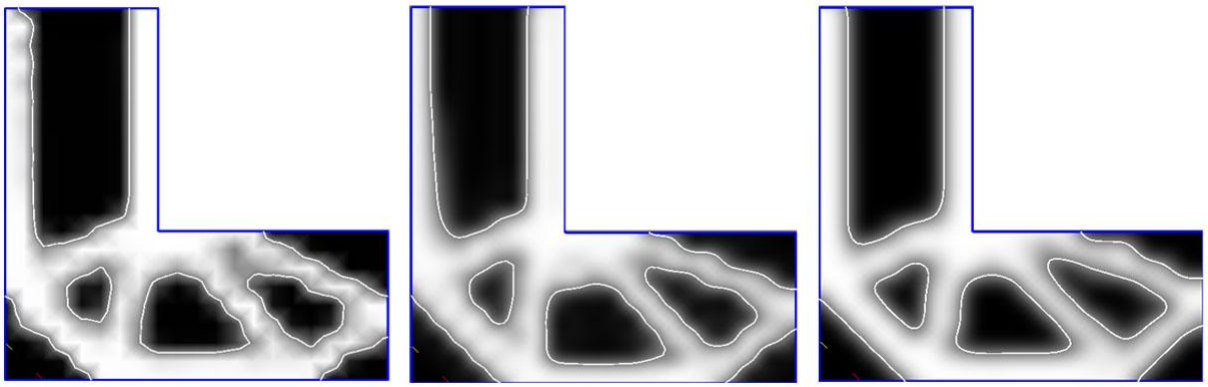

Figure 6-3 Topology results of L-shaped structure with smoothing for a mesh of 20 x 20 and volume fraction of 0.5. (a) Quad 4N elements (b) B-spline 9N elements (c) B-spline 16N elements.

The topology results of the optimal minimum compliance designs in addition with the smoothing term for a dense mesh of 70 x 70 elements are shown in Figure 6-4. The topology designs are obtained using B-spline 9 node and B-spline 16 node elements and the results compared with the results obtained using bilinear 4 node quadrilateral elements. SIMP interpolation method with the penalty parameter $p = 4$ for the density function and the allowable material volume fraction of 0.5 is used.

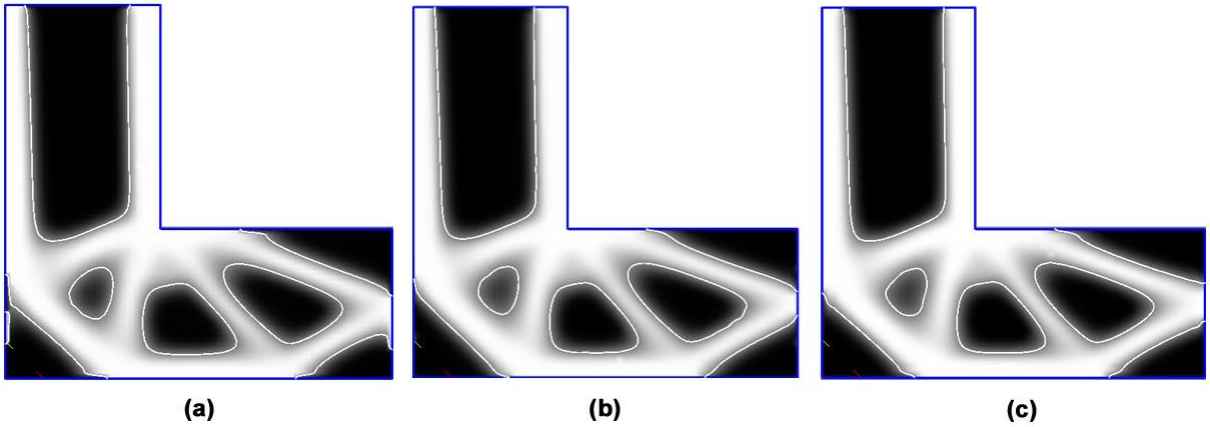

Figure 6-4 Topology results of L-shaped structure with smoothing for a mesh of 70 x 70 and volume fraction of 0.5. (a) Quad 4N elements (b) B-spline 9N elements (c) B-spline 16N elements.

It can be observed that even with the change in the size of the mesh, the inclusion of the smoothing term in the objective function yields solutions having similar topology irrespective of the type of the element used.

Mesh-Independent Results

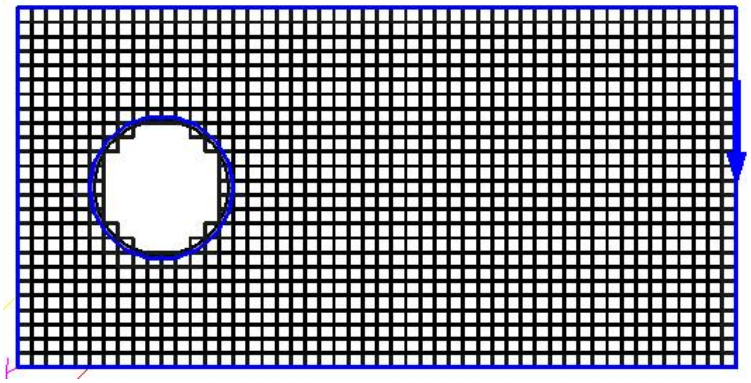

Figure 6-5 Feasible domain for a beam with a circular hole.

To study the effect of the smoothing scheme on the size of the mesh used, a cantilever beam with circular hole as a support is considered. It is often observed that the solutions for a structure with circular support are mesh-dependent and the solutions

keep varying with increased mesh refinement. Small microstructures tend to appear with the increase in mesh refinement.

The feasible domain is a rectangular domain of size 0.5 x 0.25 with a fixed circular support as shown in the Figure 6-5. A concentrated shear force is applied along the right edge of the structure. The material of the domain is assumed to be steel with modulus of elasticity equal to 200 GPa and Poisson's ratio of 0.3. A weight of 0.001 has been used for the smoothing term.

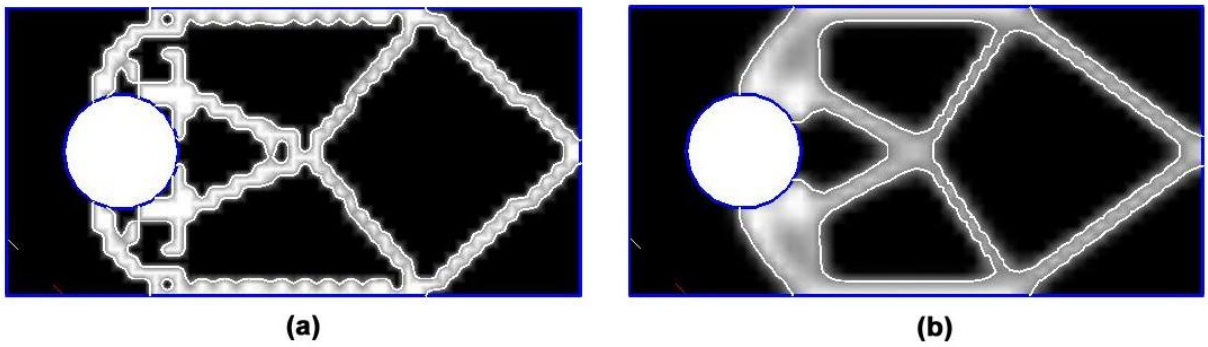

Figure 6-6 Topology results for the beam with circular hole using Q4 elements with a mesh size of 50 x 25 elements and a volume fraction of 0.8. (a) without smoothing (b) with smoothing

The topology results of the optimal designs without the smoothing scheme and using the smoothing scheme are shown in Figure 6-6. The topology designs are obtained using bi-linear 4 node quadrilateral elements with a mesh density of 50 x 25 elements. SIMP interpolation method with the penalty parameter $p = 3$ for the density function and the allowable material volume fraction of 0.8 is used. The optimal shape obtained without the smoothing scheme is not well connected and the boundaries are uneven. The shape obtained using the smoothing scheme has smooth, well-defined boundaries.

The topology results for the beam with circular hole support for different mesh densities are shown in the Figure 6-7. A weight of 0.001 has been used for the smoothing term. The results without the smoothing scheme are shown on the column on the left and the results using the smoothing scheme are shown on the column on the right. It is evident from the results that the optimal shapes obtained without the smoothing scheme are distinctly different with changes in mesh refinement. More and more members of the structures tend to appear in the final optimal topology as the mesh density increases. Figure 6-7 (e) shows the result for a mesh density of 160 x 80 elements.

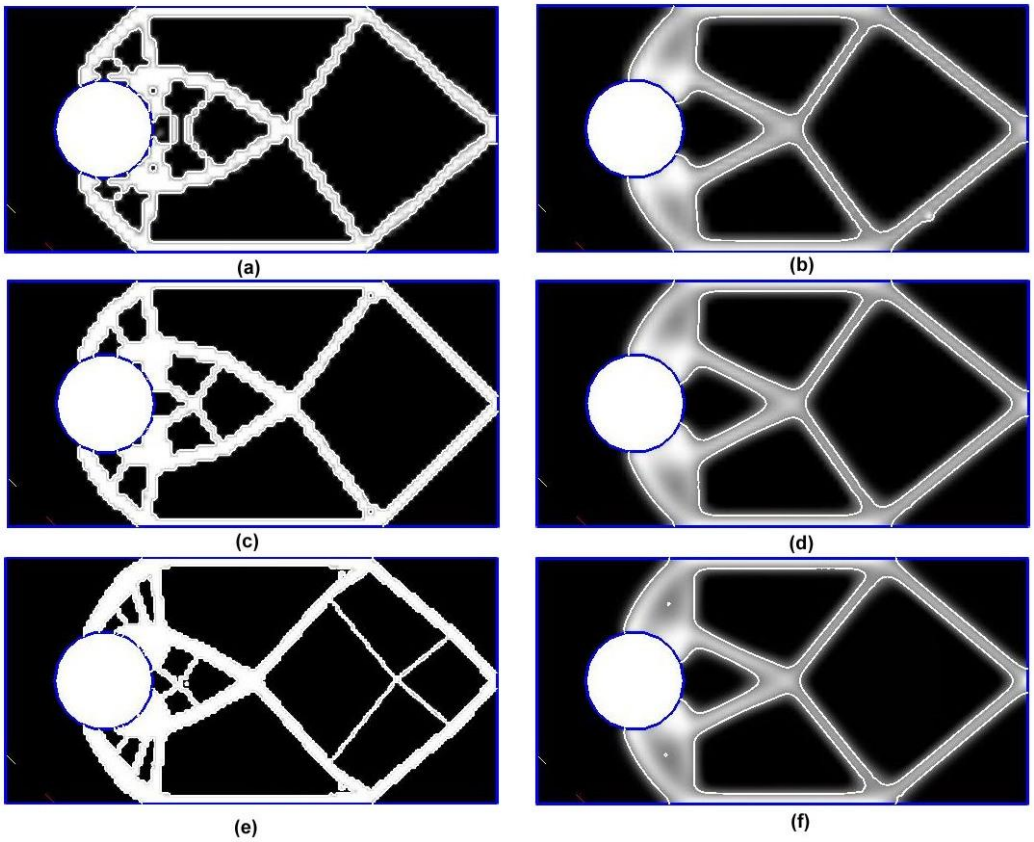

Figure 6-7 Topology results for the beam with circular hole using Q4 elements with varying mesh sizes. Left column - without smoothing, Right column - with smoothing (a), (b) 70 x 35 element mesh (c), (d) 100 x 50 element mesh (e), (f) 160 x 80 element mesh

On the other hand, the solutions obtained using the smoothing scheme are completely invariant to the changes in the mesh densities. The optimal shapes do not change with the increase in the mesh density and have extremely smooth boundaries.

Table 4-2 Compliance values for mesh independent results

Mesh density	without smoothing	with smoothing
50 x 25	0.110422	0.152871
70 x 35	0.090938	0.151540
100 x 50	0.083231	0.152363
160 x 80	0.082531	0.156277

The compliance for the mesh independent results are shown in Table 4-2 along with the compliance values without the use of the smoothing term. Although the compliance values with the smoothing scheme are a little higher, they remain almost invariant with varying sizes of mesh. On the other hand, the compliance obtained without smoothing varies with the different sizes of mesh discretization.

Thus, the use of the smoothing scheme results in obtaining mesh-independent solutions and solutions that are independent of the type of the elements used. It also helps in obtaining solutions with smooth and clearly defined boundaries.

CHAPTER 7
CONCLUSIONS

Summary

An alternative approach to represent shapes in the topology optimization process has been used. The boundaries of the structure are represented using highly smooth density function. The contours of the shape density function corresponding to a threshold value of the density are defined as the boundaries of the geometry. The nodal values of the density in the finite element model are treated as the design variables for topology optimization and the density varies continuously within the elements. The contours are either interpolated or approximated to obtain the boundaries of the geometry. Traditional finite elements such as bilinear quadrilateral elements result in final topologies that are only C^0 continuous and require extremely dense mesh to represent smooth shapes. In this thesis, B-spline finite elements are used to obtain topology results. In B-spline finite elements, the contours of the shape density function are represented using B-spline approximations. In addition, the displacement field for the structural analysis is also represented using B-spline approximations. Nodes of the B-spline elements often lie outside the element in the parameter space. Therefore, it requires a method which allows application of boundary conditions and loads even where nodes do not exist. Implicit Boundary Finite Element Method has the capability to apply boundary conditions and loads even where nodes do not exist and is used in this thesis to extend the B-spline elements for topology optimization. Quadratic and cubic B-spline finite elements are used to obtain optimal shapes and the results compared with the traditional bilinear 4-node quadrilateral elements with Lagrange interpolation functions.

B-spline elements are applied to various minimum compliance topology design problems and the results compared with the designs obtained using bilinear quadrilateral elements. B-spline elements were also applied to compliant mechanism design to design mechanisms which perform in a desired fashion. Various objective functions to generate compliant mechanism designs were studied.

Mesh discretization has been one of the important factors which influence the computational results of topology optimization problems. A new smoothing scheme to obtain solutions that are not dependent on the initial mesh discretization is introduced. The smoothing scheme is computed as an integral of square of gradient of density over the entire volume of the design domain. The smoothing term is augmented to the original objective criterion as a weighted sum in the optimization problem. Examples are shown to illustrate the use of the smoothing scheme to obtain final topologies independent of the mesh discretization.

Discussions

The interpolation or approximation of the density within each element in the finite element model allows the density to vary continuously within the elements. The displacement field and the density field are both represented using B-spline approximations for topology optimization using B-spline elements and hence the numerical instabilities due to mixed formulations in the finite element method is eliminated. Since the contours of shape density function are represented using B-spline approximations, the use of B-spline elements for topology optimization results in geometries that have smooth boundaries even with a sparse mesh discretization. In addition, the B-spline basis functions yield solutions that are C^1 or C^2 continuous in the design domain. B-spline basis have a wider span which provides an inherent smoothing

of the optimized shapes without any need for additional filters and hence the appearance of checkerboard pattern is eliminated. The computational costs incurred with the use of the B-spline elements for structural analysis are substantially higher than the quadrilateral elements and hence B-spline elements are most effective with sparse mesh densities to obtain smooth geometries.

Various objective functions for the design of compliant mechanisms which were expressed as ratios of two conflicting objectives were considered. The objective function often changed signs during the optimization process due to the fact that one of the quantities in the objective function changed sign. Since the optimization algorithm implemented in our program cannot impose inequality constraints, a non-negative constraint on the quantities in the objective function could not be imposed. Hence, an objective function which minimizes the error between actual and specified displacements at certain nodes was used to design compliant mechanisms.

The use of the new smoothing scheme provides smooth transition of density at the boundaries and therefore results in solutions that are independent of changes in the mesh discretization. The smoothing term also minimizes the number of holes that can appear in the final geometry. In addition to the mesh independent solutions, it has also been observed that the final topologies are independent of the type of the elements used for the structural analysis in the optimization process. Although the smoothing scheme yields solutions that are independent of the mesh discretization, the appropriate weight for the smoothing term is different for each structural optimization problem. The weight was derived on a trial and error basis and a specific trend was not observed in the weights used for different design problems. An intuitive method of computation of

the weight would be to use a fraction of the initial compliance of the structure as the weight. Since a particular mathematical expression to obtain the weights has not yet been derived, the use of weight for the smoothing term has been arbitrary. It has been observed that with the increase in the weight for the smoothing term, more pronounced grey areas with intermediate densities are obtained in the final topology.

Scope of Future Work

B-spline elements are currently applied to minimum compliance designs and compliant mechanism designs. Topology optimization to shell-like structures has been studied only using traditional finite elements. The extension of B-spline elements for topology optimization of shell like structures will yield smoother shapes. There are a few challenges in extending B-spline elements for topology optimization of shell-like structures. The nodal values of density can no longer be treated as design variables since the surface does not pass through the nodes in the structured mesh. Another challenge is related to the displaying of graphics for the topologies obtained using shell-like structure. Topology optimization using B-spline elements can be extended to three dimensional structures since the approach is quite similar to planar structures. The difficulty associated with the three dimensional structure is again related to the graphics display of the topologies. B-spline elements can also be extended for topology optimization with stress constraints. One of the challenges related to topology optimization with stress constraints is that the number of constraints becomes too large to handle. For example, imposing stress constraints at all the nodes in the design domain results in substantial increase in the computational costs as the stresses have to be recomputed during each iteration of the optimization process. Topology

optimization in can be also applied to generate optimal shapes with a specified mode shape of vibration.

LIST OF REFERENCES

[1] Bendsøe MP, Kikuchi N. Generating optimal topologies in structural design using a homogenization method. Computer methods in applied mechanics and engineering 1988; 71: 197-224.

[2] Bendsøe MP, Sigmund O. Topology optimization theory, methods and applications. Springer; 2003.

[3] Kumar AV, Gossard DC. Geometric modeling for shape and topology optimization. In: Proc. of Geometric modeling for product realization; 1992.

[4] Burla RK, Kumar AV. Implicit boundary method for analysis using uniform B-splines basis and structured grid. International journal for numerical methods in engineering 2008; 76: 1993-2028.

[5] Haftka RT, Gurdal Z, Kamat MP. Elements of structural optimization. Kluwer academic publishers; 1990.

[6] Kirsch U. Structural optimization: fundamentals and applications. Springer; 1993.

[7] Yunliang D. Shape optimization of structures: a literature survey. Computers and structures 1986; 24(6): 985-1004.

[8] Zienkiewicz OC, Campbell JS. Shape optimization and sequential linear programming. In: Gallagher RH, Zienkiewicz OC, editors. Optimum Structural Design. John Wiley; 1973.

[9] Vanderplaats GN. Numerical methods for shape optimization: an assessment of the state of the art. In: Atrek E, Gallagher RH, Ragsdell KM, Zienkiewicz OC, editors. New direction in optimum structural design. John Wiley; 1984.

[10] Haug EJ, Choi KK, Hou JW, Yoo YM. A variational method for shape optimal design of elastic structures. In: Atrek E, Gallagher RH, Ragsdell KM, Zienkiewicz OC, editors. New direction in optimum structural design. John Wiley, 1984.

[11] Haftka RT, Grandhi RV. Structural shape optimization–a survey. Computer methods in applied mechanics and engineering 1985; 57: 91-106.

[12] Chapman CD, Saitou K, Jakiela MJ. Genetic algorithm as an approach to configuration and topology design. Journal of mechanical design 1994; 116: 1005-1012.

[13] Ohsaki M. Genetic algorithm for topology optimization of trusses. Computers and structures 1995; 57(2): 219-225.

[14] Kaveh A, Kalatjari V. Topology optimization of trusses using genetic algorithm, force method and graph theory. International journal for numerical methods in engineering 2003; 58: 771-791.

[15] Wang SY, Tai K. Structural topology design optimization using genetic algorithms with a bit-array representation. Computer methods in applied mechanics and engineering 2005; 194: 3749-3770.

[16] Xie YM, Steven GP. A simple evolutionary procedure for structural optimization. Computers and structures 1993; 49: 885-896.

[17] Chu DN, Xie YM, Hira A, Steven GP. On various aspects of evolutionary structural optimization for problems with stiffness constraints. Finite elements in analysis and design 1997; 24: 197-212.

[18] Zhou M, Rozvany GIN. On the validity of ESO type methods in topology optimization. Structural and multidisciplinary optimization 2001; 21: 80-83.

[19] Ansola R, Vegueria E, Canales J, Tarrago JA. A simple evolutionary topology optimization procedure for compliant mechanism design. Finite elements in analysis and design 2007; 44: 53-62.

[20] Wang MY, Wang X, Guo D. A level set method for structural topology optimization. Computer methods in applied mechanics and engineering 2003; 192: 227-246.

[21] Rong JH, Liang QQ. A level set method for topology optimization of continuum structures with bounded design domains. Computer methods in applied mechanics and engineering 2008; 197: 1447-1465.

[22] Wang SY, Lim KM, Khoo BC, Wang MY. An extended level set method for shape and topology optimization. Journal of computational physics 2007; 221: 395-421.

[23] Cheng G, Olhoff N. An investigation concerning optimal design of solid elastic plates. International journal of solids and structures 1981; 16: 305-323.

[24] Cheng G, Olhoff N. Regularized formulation for optimal design of axisymmetric plates, International journal of solids and structures 1982; 18: 153-170.

[25] Kohn RV, Strang G. Optimal design and relaxation of variational problems. Communications in pure applied mathematics 1986; 39: 113-137 (Part I), 139-182 (Part II), 333-350 (Part III).

[26] Bendsøe MP. Optimal shape design as a material distribution problem. Structural and multidisciplinary optimization 1989; 1: 193-202.

[27] Rozvany GIN, Zhou M, Sigmund O. Topology optimization in structural design. In: Adeli H, editors. Advances in design optimization. Chapman and hall; 1994.

[28] Yang RJ, Chuang CH. Optimal topology design using linear programming. Computers and structures 1994; 52(2): 265-275.

[29] Jog CS, Haber RB. Stability of finite element models for distributed-parameter optimization and topology design. Computer methods in applied mechanics and engineering 1996; 130: 203-226.

[30] Jog CS, Haber RB, Bendsøe MP. Topology design with optimized, self-adaptive materials. International journal for numerical methods in engineering 1994; 37: 1323-1350.

[31] Diaz A, Sigmund O. Checkerboard patterns in layout optimization. Structural and multidisciplinary optimization 1995; 10: 40-45.

[32] Sigmund O. A 99 line topology optimization code written in matlab. Structural multidisciplinary optimization 2001; 21: 120-127.

[33] Kumar AV, Gossard DC. Synthesis of optimal shape and topology of structures. Journal of mechanical design Trans of ASME 1996; 118: 68-74.

[34] Kumar AV, Padmanabhan S, Burla R. Implicit boundary method for finite element analysis using non-conforming mesh or grid. International journal for numerical methods in engineering 2008; 74: 1421-1447.

[35] Kumar AV. A sequential optimization algorithm using logarithmic barriers: applications to structural optimization. Journal of mechanical design 2000; 122: 271-277.

[36] Midha A, Norton TW, Howell LL. On the nomenclature, classification, and abstractions of compliant mechanisms. Journal of mechanical design 1994; 116: 270-279.

[37] Her I, Midha A. A compliance number concept for compliant mechanisms, and type synthesis. Journal of mechanisms, transmissions, and automation in design 1987; 109(3): 348-355.

[38] Murphy MD, Midha A, Howell LL. The topological synthesis of compliant mechanisms. Mechanism and machine theory 1996; 31(2): 185-199.

[39] Howell LL, Midha A. A method for the design of compliant mechanisms for small-length flexural pivots. Journal of mechanical design 1994; 116: 280-290.

[40] Howell LL, Midha A. A loop-closure theory for the analysis and synthesis of compliant mechanisms 1996; 118: 121-125.

[41] Howell LL, Midha A, Norton TW. Evaluation of equivalent spring stiffness for use in a pseudo-rigid-body model of large-deflection compliant mechanisms. Journal of mechanical design 1996; 118: 126-131.

[42] Ananthasuresh GK, Kota S, Gianchandani Y. A methodical approach to the synthesis of micro compliant mechanisms. In: Technical digest of Solid-state sensor and actuator workshop 1994: 189-192.

[43] Ananthasuresh GK, Kota S. Designing compliant mechanisms. Mechanical engineering 1995; 117(11): 93-96.

[44] Ananthasuresh GK, Kota S, Kikuchi N. Strategies for systematic synthesis of compliant MEMS. In: Proc. of ASME winter annual meeting 1994; 55(2): 677-686.

[45] Sigmund O. Some inverse problems in topology design of materials and mechanisms. In: Proc. of IUTAM symposium on optimization of mechanical systems 1995. p. 277-284.

[46] Larsen UD, Sigmund O, Bouwstra S. Design and fabrication of compliant micromechanisms and structures with negative Poisson's ratio In: Proc. of IEEE 9th annual international workshop on micro electro mechanical systems 1996. p. 11-15.

[47] Sigmund O. On the design of compliant mechanisms using topology optimization. Mechanics of structures and machines 1997; 25(4): 493-524.

[48] Lau GK, Du H, Lim MK. Use of functional specifications as objectives in topological optimization of compliant mechanism. Computer methods in applied mechanics and engineering 2001; 190: 4911-4928.

[49] Bruns TE, Tortorelli DA. Topology optimization of non-linear elastic structures and compliant mechanisms. Computer methods in applied mechanics and engineering 2001; 190: 3443-3459.

[50] Pedersen CBW, Buhl T, Sigmund O. Topology synthesis of large-displacement compliant mechanisms. International journal for numerical methods in engineering 2001; 50: 2683-2705.

[51] Frecker MI, Ananthasuresh GK, Nishwaki S, Kikuchi N, Kota S. Topological synthesis of compliant mechanisms using multi-criteria optimization. Journal of mechanical design 1997; 119: 238-245.

[52] Nishiwaki S, Frecker MI, Min S, Kikuchi N. Topology optimization of compliant mechanisms using the homogenization method. International journal for numerical methods in engineering 1998; 42(3): 535-559.

[53] Frecker MI, Kikuchi N, Kota S. Topology optimization of compliant mechanisms with multiple outputs. Structural and multidisciplinary optimization 1999; 17(4): 268-278.

[54] Kota S, Joo J, Li Z, Rodgers SM, Sniegowski J. Design of compliant mechanisms: applications to MEMS. Analog integrated circuits and signal processing 2001; 29(1): 7-15.

[55] Chen S, Wang MY, Liu AQ. Shape feature control in structural topology optimization. Computer aided design 2008; 40: 951-962.

[56] Sigmund O, Peterson J. Numerical instabilities in topology optimization: a survey on procedures dealing with checkerboards, mesh-dependencies and local minima. Structural multidisciplinary optimization 1998; 16: 68-75.

[57] Zhou M, Shyy YK, Thomas HL. Checkerboard and minimum member size control in topology optimization Structural multidisciplinary optimization 2001; 21: 152-158.

BIOGRAPHICAL SKETCH

Anand Parthasarathy hails from a city called Chennai in the southern part of India. He graduated his high school in 2001 from Sri Ahobila Math Oriental High School, Chennai, India. He graduated with a bachelor's degree in mechanical engineering in 2005 from the College of Engineering Guindy, Chennai, India. He received his master's degree in mechanical engineering in the spring of 2010 from the University of Florida, Gainesville, USA. His areas of interests include finite element methods, structural optimization, computer aided design and modeling, applications of computer programming in mechanical engineering.